Environmental Science and Pollution Research (2024) 31:42640–42671
https://doi.org/10.1007/s11356-024-34021-2

REVIEW ARTICLE

Emerging trends in hydrogen and synfuel generation: a state-of-the-art review

Mansur Alhassan[1,3] · Aishah Abdul Jalil[1,2] · Abdelrahman Hamad Khalifa Owgi[1] · Muhamed Yusuf Shahul Hamid[1] · Mahadi Bin Bahari[4] · Thuan Van Tran[1,5] · Walid Nabgan[6] · Abdul Hakim Hatta[1] · Nur Farahain Binti Khusnun[1] · Abiodun Abdulhameed Amusa[1,2] · Bemgba Bevan Nyakuma[7]

Received: 15 July 2023 / Accepted: 13 June 2024 / Published online: 21 June 2024

Abstract

The current work investigated emerging fields for generating and consuming hydrogen and synthetic Fischer-Tropsch (FT) fuels, especially from detrimental greenhouse gases, CO_2 and CH_4. Technologies for syngas generation ranging from partial oxidation, auto-thermal, dry, photothermal and wet or steam reforming of methane were adequately reviewed alongside biomass valorisation for hydrogen generation, water electrolysis and climate challenges due to methane flaring, production, storage, transportation, challenges and opportunities in CO_2 and CH_4 utilisation. Under the same conditions, dry reforming produces more coke than steam reforming. However, combining the two techniques produces syngas with a high H_2/CO ratio, which is suitable for producing long-chain hydrocarbons. Although the steam methane reforming (SMR) process has been industrialised, it is well known to consume significant energy. However, coke production via catalytic methane decomposition, the prime hindrance to large-scale implementation of these techniques for hydrogen production, could be addressed by coupling CO with CO_2 conversion to alter the H_2/CO ratio of syngas, increasing the reaction temperatures in dry reforming, or increasing the steam content fed in steam reforming. Optimised hydrogen production and generation of green fuels from CO_2 and CH_4 can be achieved by implementing these strategies.

Keywords Dry reforming · Steam reforming · Partial oxidation · Auto-thermal reforming · Photothermal conversion · Fischer-Tropsch synthesis

Responsible Editor: Ta Yeong Wu

✉ Aishah Abdul Jalil
aishahaj@utm.my

[1] Faculty of Chemical and Energy Engineering, Universiti Teknologi Malaysia, 81310 Skudai, Johor, Malaysia

[2] Centre of Hydrogen Energy, Institute of Future Energy, Universiti Teknologi Malaysia, 81310 Skudai, Johor, Malaysia

[3] Department of Chemistry, Sokoto State University, P. M. B 2134, Airport Road, Sokoto, Nigeria

[4] Faculty of Science, Universiti Teknologi Malaysia, 81310 Skudai, Johor, Malaysia

[5] Institute of Applied Technology & Sustainable Development, Nguyen Tat Thanh University, 298-300A Nguyen Tat Thanh, District 4, HCMC 755414, Viet Nam

[6] Departament d'Enginyeria Química, Universitat Rovira i Virgili, Av Països Catalans 26, 43007 Tarragona, Spain

[7] Department of Chemical Sciences, Faculty of Science and Computing, Pen Resource University, P.M.B 0198, Gombe, Gombe State, Nigeria

Abbreviations

AE	Anionic exchange
AR	Air reactor
ATF@PCM	ATF suspension fixed Phase change microcapsules
ATR	Auto-thermal reforming of methane
ATR@PCM	ATR suspension fixed Phase change microcapsules
BM	Ball milling
BR	Boudouard reaction
CCS	Carbon capture and storage
CCU	Carbon capture and utilisation
CCUS	carbon capture utilisation and storage
CH_4	Methane
CLH	Chemical looping hydrogen
CO	Carbon monoxide
CO_2	Carbon (IV) oxide
COG	Coke oven gas
CPO	Catalytic partial oxidation
CSR	Catalytic steam reforming

CSDRM	Combined steam and dry reforming of methane
DME	Dimethyl ether
DR	Dry reforming
DRM	Dry reforming of methane
ECR	Electrochemical catalytic reforming
EHCs	Energetic hot carriers
FR	Fuel reactor
FT	Fischer-Tropsch
GTC	Gas to chemicals
GTL	Gas to liquids
GTP	Gas to power
H_2	Hydrogen
H_2O	Water
ICI	Incipient impregnation
IM	Impregnation
IWI	Incipient wet impregnation
kJ mol^{-1}	Kilo Joule per mole
MR	Methane reforming
OC	Oxygen carrier
PAHs	Polycyclic aromatic hydrocarbons
PCP	Precipitation
PH	Post-hydrolysis
POX	Partial oxidation
POXM	Partial oxidation of methane
PSA	Primary swing adsorption
PTR	Photothermal reforming of methane
RFG	Recycled flue gas
RWGS	Reverse water gas shift
SI	Sequential impregnation
SOFC	Solid oxide fuel cell
SR	Steam reforming
SRE	Steam reactor
SRM	Steam reforming of methane
TOF	Turnover frequency
WGS	Water gas shift
WI	Wet impregnation

Introduction

The world's population continues to expand at a rapid rate, leading to a significant increase in energy demands. This demand is even higher than the population growth itself (Abdelkareem et al. 2022). The depletion of fossil fuels, which is influenced by factors such as geographical distribution and extraction accessibility, adds to the challenge (Sagar et al. 2024). Moreover, heavy reliance on fossil fuels contributes to the accumulation of greenhouse gases like carbon (IV) oxide (CO_2) in the atmosphere, which is the primary cause of global warming. Consequently, there is an urgent need to explore alternative, environmentally sustainable energy sources (Cao et al. 2024). Given this pressing need, there is a growing interest in alternative energy sources driven by both the rising global energy demand and concerns about the carbon footprint of fossil fuels (Lara Sandoval et al. 2024). Amongst the potential options, hydrogen stands out as a promising and environmentally friendly fuel source (Singh et al. 2017; Abdelkareem et al. 2022). Projections indicate that global demand for hydrogen energy across various industries will increase by approximately 400 Mt/year over the next five decades (Ighalo and Amama 2024).

Syngas (a mixture of hydrogen (H_2) and carbon monoxide (CO)) is an intermediate feedstock used to produce a variety of fuels and chemicals, including H_2, methanol, FT fuels, dimethyl ether (DME) and ethanol (Peña et al. 1996; Elvidge et al. 2015; Taherian et al. 2021; Jin et al. 2021). Its efficient commercialisation is gaining significant attention worldwide. H_2 is the perfect upcoming clean energy alternative (Puangpetch et al. 2009; Kong et al. 2019; Araiza et al. 2021; Li et al. 2022). Over the past few decades, emissions from burning fossil fuels like coal, oil, CO_2 and natural gas have contributed to a steady, rapid increase in global warming, resulting in severe environmental pollution (Wang et al. 2018b; Qingli et al. 2021; Nabgan et al. 2022; Sasidhar et al. 2022). A fossil fuel-based source of energy is non-renewable (Qingli et al. 2021); therefore, the search for alternative, cleaner and eco-friendlier forms of energy has gained significant attention in recent years (Makertiharta et al. 2017; Alhassan et al. 2022; Lee et al. 2022).

Biodiesel is an excellent choice for utilising the potential of biomass. Globally, more than 27 million metric tonnes of biodiesel are generated each year. Glycerine (10% of which is a by-product) may contain water, free fatty acids, manufacturing residues and trace amounts of heavy metals, impacting its purity and suitability for specific uses. Before being used, the crude glycerine must be refined. To produce hydrogen from biomass, two thermochemical processes are available. The first is biomass gasification, while the second is catalytic steam reforming of biomass pyrolysis oil (also known as bio-oil) (Wang et al. 2014). Biomass steam reforming (SR) via pyrolysis, the second method, which involves hydrogen production via biomass pyrolysis (SR of bio-oil), is a more cost-effective alternative due to the high bio-oil yield and mobility. Nonetheless, the challenge of purification associated with the techniques results in a significant price increase (Wang et al. 2014; Chen et al. 2017; Yi et al. 2023).

Most of the nearly 210 billion Nm^3 of coke oven gas (COG) by-products from the metallurgical sector are either burned directly as fuel or discharged directly into the atmosphere, squandering energy and harming the environment. Due to its high hydrogen content (48–55 mol % H_2), it has been described as one of the raw materials most likely to attain large-scale commercial H_2 production in the short and medium terms. Physical separation technologies

like pressure swing adsorption (PSA) are used to extract H_2 from COG. Still, this process also removes other components like CO, methane (CH_4), tar and hydrocarbons like polycyclic aromatic hydrocarbons (PAHs), xylene and toluene, whose further separation takes up large amounts of ammonia and contaminates water sources (Xie et al. 2017).

It has been proposed that chemical looping hydrogen (CLH) technology is an innovative and viable method of manufacturing H_2 incorporating CO_2 segregation, good product quality and high efficiency. The steam or fuel reactor (SRE/ FR) and the air reactor (AR) are the most common reactors in a CLH. In the steam reactor (SR), steam oxidises the reduced oxygen carrier (OC) to produce high-purity H_2. The challenges for the process include fuel conversion, steam conversion, heat duty and the optimum ratios of OC to COG, steam to OC and air to OC (Xiang and Zhao 2018). The splitting of water into H_2 and oxygen ($O_{2)}$ using solar energy is another possibility being considered since H_2 gas is a powerful energy source because of its high gravitational energy density and is environmentally benign via near-zero greenhouse gas production (Tolod et al. 2016).

Typically, large-scale H_2 generation is mainly accomplished via fossil fuel reforming and water electrolysis, even though this latter technique accounts for just 5 % of total H_2 production (Meloni et al. 2020). Photocatalytic water splitting is amongst the most recent techniques for generating H_2. It allows the conversion of solar energy to chemical energy, enabling the use of solar energy and water. This is a viable approach for moving from a fossil fuel economy to a green, hydrogen-powered one (Puangpetch et al. 2009; Sayed et al. 2019). The SR of CH_4 (SRM), partial oxidation (POX), dry reforming (DRM) and auto-thermal reforming (ATR) are examples of fuel reforming processes. SRM is the oldest and most practical method for converting CH_4 to H_2 amongst the reforming processes. It is typically described as the consequence of (Eq. (1)) and (Eq. (2)) and has a high H_2/CO ratio of 3:1; working temperatures over 700 °C are needed for this reforming reaction, and steam-to-methane ratios of 2.5 to 3.0 are often used to minimise coke formation (Matas Güell et al. 2011; Yentekakis et al. 2021).

According to a recent report by Meloni and co-researchers (Meloni et al. 2020), the most used catalyst for SRM is Ni supported over ceramic oxides or oxides of metallic or metalloid elements. Other group VIII metals are active, although they have specific disadvantages; for instance, Fe oxidises rapidly, Co cannot survive steam partial pressures, and precious metals (Rh, Ru, Pt and Pd) are outrageously costly for practical use. Supports often employed include alumina (Zhang et al. 2017; Pirshahid et al. 2023), magnesia (Bian et al. 2016; Alabi et al. 2020), calcium aluminate (Batuecas et al. 2021; Zhang et al. 2024) and magnesium aluminate (Alabi et al. 2020).

The catalytic POX is more energy efficient due to its rapid kinetics and exothermic nature, eliminating the need for huge reactors and significant quantities of superheated steam. Furthermore, the stoichiometry of POX (6) produces a synthesis gas with an H_2/CO ratio of 2:1, allowing its direct use for methanol or FT synthesis without further adjustment. However, the need for pure O_2 and the risk of explosion are associated problems in addition to the seldom-required adjustment of the product ratio (Arku et al. 2018; Chen et al. 2020).

Because of its capacity to absorb two greenhouse gases, hydrogen generation from DRM has garnered a lot of interest in recent years. CH_4 and CO_2 (Eq. (1)) generate lucrative feedstocks (syngas) with a better H_2/CO ratio, which is required as a highly valued feedstock for FT synthesis and methanol production (Afzal et al. 2020; Li et al. 2021; Ibrahim et al. 2022). Again, nickel catalysts supported by various metal oxides like ZrO_2, Al_2O_3, MgO, CeO_2 or La_2O_3 have been widely used in DRM due to their relatively high catalytic activity and low cost (Charisiou et al. 2016; Goula et al. 2017; Chaudhary et al. 2020; Ibrahim et al. 2022).

The ATR method for figuring out the value of methane is an important part of making syngas by combining adiabatic (SR) and non-catalytic (POX) processes. As a result of the sintering, production and deposition of coke, the activity of Ni catalysts, which are frequently used in this process, is diminished. Consequently, they require support from metal oxides such as CeO_2 (Song et al. 2016; Araiza et al. 2021; Zhang et al. 2023) and SiO_2 (Nath et al. 2022; Alhassan et al. 2024).

This review compares the various natural gas reforming processes, especially the potential for their implementation on an industrial scale for valuable feedstock, energy and hydrogen production; discusses the need for hydrogen-driven energy processes, utilisation, storage and transportation of CO_2; and the impacts of flared natural gas. Cutting the 300 to 400 million tonnes of CO_2 released by methane flaring is also addressed here. Novelties at each methane reforming method are well summarised, and a combination of wet and dry reforming perspectives, world energy supply and fuel-gasifier interaction from combustion, gasification, pyrolysis and drying zones was classified into oxidation, methanation, non-coke side reactions and coke side reactions.

Review novelty and objective

Considering the various challenges associated with CO_2 emissions, numerous research institutions have recently focused on valorising CO_2 into fuels and chemicals, commonly called carbon capture and utilisation (CCU). This approach is recognised as a multidimensional method. In

addition to its environmental and health advantages, the process of CO_2 upgrading holds promise for addressing the challenges associated with depleting energy resources and uneven distribution. The main objectives of this study were to comprehensively assess and examine recent advancements in catalytic technologies employed for converting CH_4 and CO_2 into chemically useful compounds and energy resources. Hydrogen emissions are environmentally beneficial because, when combined with oxygen in fuel cells, they only produce water vapour. The production of hydrogen through electrolysis, which is powered by renewable energy, offers a carbon-free process. Hydrogen has a wide range of applications and can replace fossil fuels in transportation, manufacturing and energy storage. This provides a promising solution to the environmental problems caused by conventional fuels.

Sources types and technologies to produce hydrogen

Hydrogen is an efficient energy type and has now been identified as an energy carrier that can be obtained from both renewable and non-renewable sources. However, over 70% of existing technologies to produce H_2 are based on reforming natural gas. However, reports from (Taylor and Balat 2008; Howarth and Jacobson 2021) argue that, thus far, hydrocarbon reformation, specifically methane, produces more than 96 % of H_2 from fossil fuels like coal, natural gas and petroleum. Hydrogen can dramatically lessen the environmental damage caused by fossil fuels compared to other fuels (Avci and önsan 2018).

Figure 1 provides a comprehensive overview of energy production processes and technologies that are essential for sustainable energy transitions. Figure 1A to D provide existing data regarding fuel energy demand, biomass energy demand and total energy makeup, while section E is divided into three main parts that cover pathways involving fossil fuel resources, biomass/waste utilisation and water splitting for hydrogen production. The section (1E) focuses on the utilisation of fossil fuel resources. It showcases methods such as natural gas conversion and coal gasification with carbon capture, utilisation and storage (CCUS). These technologies highlight strategies for mitigating carbon emissions while making use of existing fossil fuel infrastructure. The next segment highlights biomass and waste utilisation. It illustrates pathways for converting organic materials into energy sources. Technologies such as biomass conversion and waste-to-energy processes demonstrate the potential to reduce dependency on fossil fuels while addressing waste management challenges.

Finally, the section explains various techniques for hydrogen production through water splitting. These techniques include direct water splitting, high-temperature electrolysis and low-temperature electrolysis, each offering unique advantages and contributing to the development of sustainable hydrogen economies. Production of H_2 has been reported via numerous routes, amongst those presented in Fig. 1E: (i) low-carbon pathways utilising a variety of domestic resources, including fossil fuels; biomass conversion and waste to energy technologies, which mostly require biological processes such as anaerobic digestion and the action of microorganisms; (ii) CCUS and (iii) photoelectrochemical splitting of water into hydrogen and oxygen using either nuclear energy or renewable sources such as wind, solar, geothermal and hydroelectric power (Dutta and Vaidyalingam 2003; Lu et al. 2017; Sittipunsakda et al. 2021).

Amongst the production technologies, biomass conversion in anaerobic digesters is less efficient as they consume more time, require extensive infrastructure and inevitably must be subjected to several cleaning processes. Even though producing green hydrogen requires a feedstock that is entirely renewable and has as little carbon footprint as feasible, there are evident records in the literature (Cuéllar-Franca and Azapagic 2015; Arku et al. 2018; Xu et al. 2020) that declare that the combined impact of the method for fuel production and the extent of waste generation are critical factors for its classification. Accordingly, based on the source of production and method of separation, H_2 may be classified as brown or black (produced via pyrolysis and gasification of carbonaceous materials like coal, etc.); green (produced majorly from wind, solar, tidal, or via electrolysis, water splitting, stored as an energy vector, transferrable in space and time); blue (a low-carbon H_2 produced mainly via SR with an effective cost-benefit, product storage via CCS and minimisation of pollution); grey (in resemblance to the blue hydrogen, but where emissions from the process are released directly into the atmosphere) and turquoise in which case, CH_4 is cracked from a temperature above 600 °C to about 1200–1400 °C, generating solid coke and H_2 gas (Menon and Selvakumar 2017; Howarth and Jacobson 2021).

As reported by (Osman et al. 2022) and shown in Fig. 2, the production, safety, storage, utilisation and upgrading of H_2 were highlighted. Fuel production for transportation, power generation, the production of nitrogen fertiliser by the Odda process and NH_3 production, industrial metallurgical processes and the production of hydrocarbon fuels have been amongst the most significant uses of hydrogen. Importantly, hydrotreating processes get rid of the stubborn carcinogenic heteroatoms (N, O, S, F, etc.) in the oil pool. For example, denitrogenation gets rid of the extra nitrogen molecules that stop the acidic sites on conversion catalyst molecules from working, which makes the crude oil fractions undesirable. There

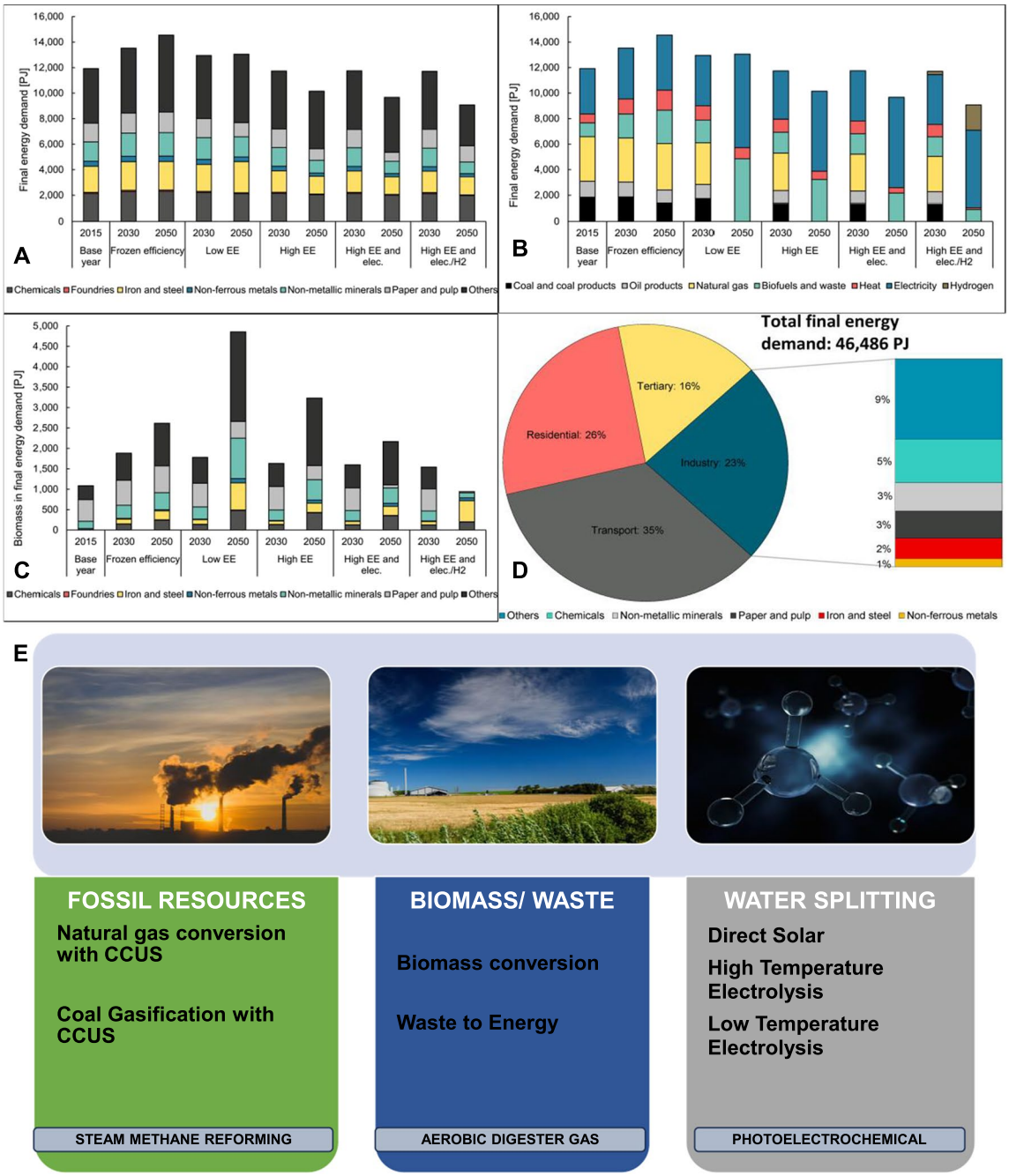

Fig. 1 Final energy demand by scenario by industrial sub-sector (**A**); energy demand scenario by fuel type (**B**); biomass consumption in energy demand (**C**) and **D** total final energy demand per energy sector (EU27 + UK), reused with permission from (Johannsen et al. 2023) and **E** Main Techniques to produce hydrogen

are corrosive nitrogen compounds; hence, natural oils above 0.25 wt % are removed during refining. Hydrodeoxygenation and hydrodesulphurisation are other industrial processes that take up a lot of H_2. Hydrotreatment also ensures the removal of inherent carcinogenic and toxic compounds of sulphur, which cause the sourness of crude. Sulphur is removed from fuels during refining to comply with laws to decrease sulphur-related air pollution. Water, minerals and other pollutants are also found in crude oil. If not removed, these salts and heavy metals produce acids, corroding downstream process equipment when heated. Oxygen dispersion in petroleum fractions induces gum development in different reactors and pipelines in refinery operations, resulting in clogging and loss of equipment efficiency (Verstraete et al. 2007; Ahmad et al. 2011; Sbaaei and Ahmed 2018).

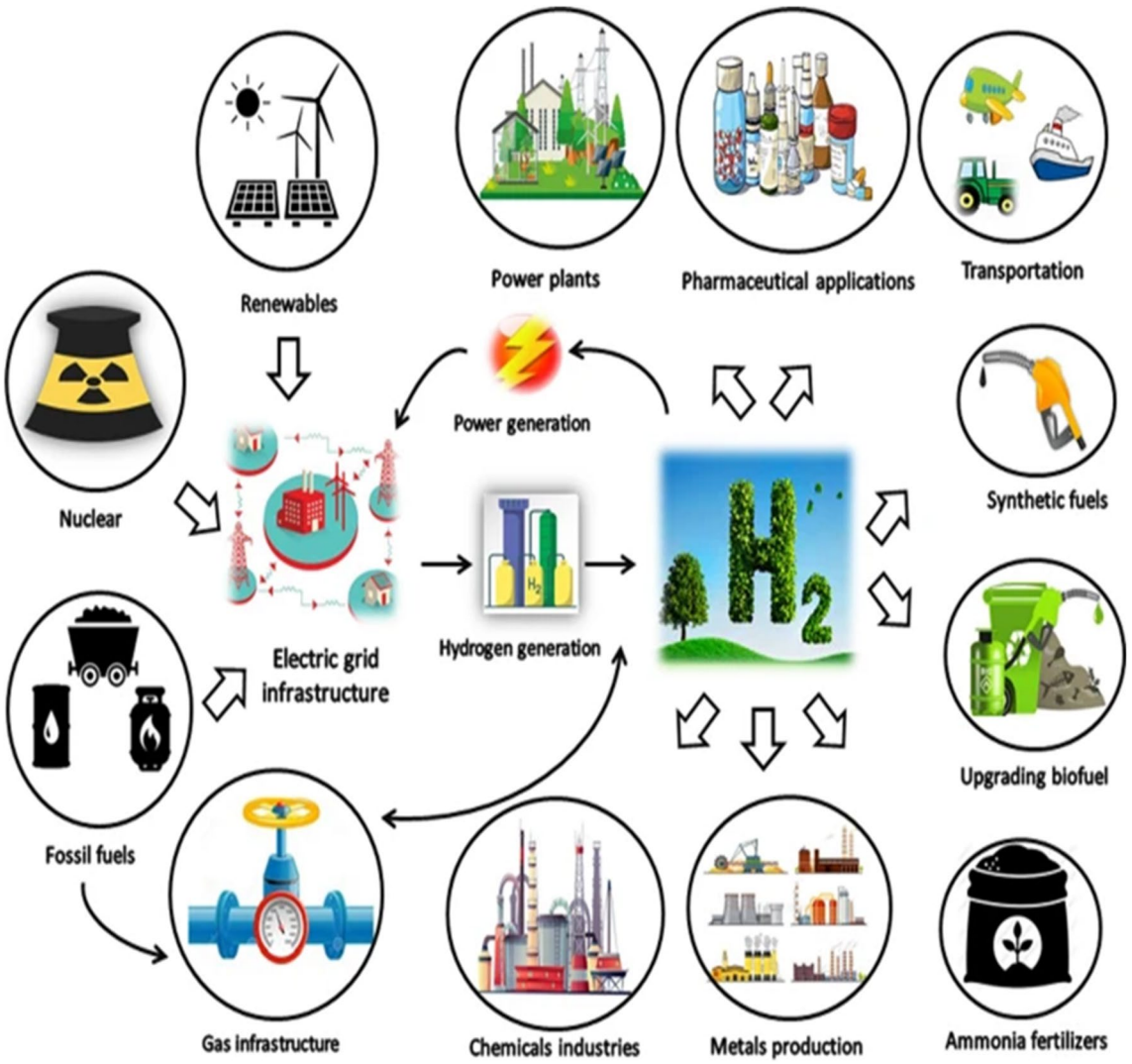

Fig. 2 Routes for hydrogen production, conversion and applications. Copied from Osman et al. (2022) with creative commons licence permission

Highlight of published data, author keywords and hydrogen production

The prevalence of techniques in the literature emphasizing the need for a switch to more green energy sources with less negative potential for the environment cannot be overemphasised (Aw et al. 2014; Papageridis et al. 2016; Alhassan et al. 2019; Ahmed et al. 2020). Unarguably, sufficient data has been published addressing the critical issues of production, safety, storage, utilisation, photoproduction, CH_4 pyrolysis, SR and other related terms, which are presented in Fig. 3. The search terms "hydrogen production" and "energy generation" were typed in the search box on the Web of Science (WoS) interface under all fields. The outcome was used to generate the plain text file from which the cluster shown in Fig. 3 was generated. The author keywords of 1000 publications were refined to 15 or more appearances, indicating that only the keywords that satisfy the threshold appear in the cluster. Interestingly, the closest terms to H_2 production are CH_4 conversion, thermal decomposition, energy generation, biomass gas systems, visible light and water gas from the top; storage, kinetics, electrolysis, catalysts and temperature from the left; and evolution, decomposition, optimisation, visible light irradiation and photo-fermentation from the bottom.

Hydrogen production for energy and natural gas conversion has been a serious and important aspect over the last 2 decades. Based on an explanation for similar clusters in the studies (Alhassan et al. 2022; Hatta et al. 2023), the figure emphasised that photo-fermentation has not been established in the literature as much as the methane conversion route. This is evident from the text size of the keyword and its

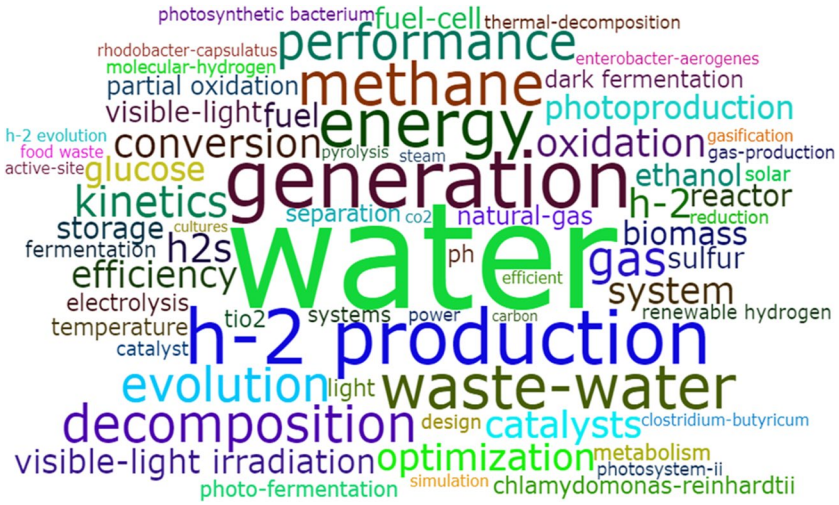

Fig. 3 Cluster displaying the relationship between the strongest author keywords. Generated using R-studio from plain text file extracted from the WoS

closeness to the other keywords. Astonishingly, the generation of natural gas as an energy alternative from food waste, especially via the incorporation of the action of microorganisms, is also shown by the appearance of fermentation, food waste and renewable H_2 in the cluster.

Opportunities and challenges in CO_2 utilisation for green fuels

Increased CO_2 emissions are the principal cause of global warming, an unavoidable threat that has attracted international attention (Bruhn et al. 2016; He and Liu 2017). Carbon cycles exist in bulk between the continental environment and the ocean. Global CO_2 emissions surpassed 9.68 billion metric tonnes in 2014, 60% of which remained in the atmosphere, according to BP world energy data (British Petroleum 2021). CO_2 output must be reduced by 60–70% to ensure equilibrium as nature absorbs 3 billion metric tonnes of carbon every year. As of October 2021, the average CO_2 concentration had shot up to roughly 414 ppm, an increase of approximately 47.86% relative to pre-industrial revolution levels (280 ppm). This dramatic increase in CO_2 concentration led to further global climate change. According to the Goddard Centre for Space Studies, the land-ocean temperature index (°C) has grown from − 0.16 °C in 1880 to 1.02 °C in 2020 (Chai et al. 2022).

Supercritical CO_2 functions in polymerisation, refrigeration and as a working fluid. Subsequently, the absorption, utilisation and valorisation of CO_2 are needed to combat pollution and global warming caused by their expanding sources. By 2030, process advancements should cut post-combustion capture costs from 52 to around 25–30 USD/tonne (Valluri et al. 2022). Similarly, its application in iron and steel production includes iron ore extraction, usually improved by flotation or magnetic separation, pelletisation for transport into the blast boiler, reduction into pig iron and steel refining using a basic oxygen boiler or electric arc boiler. Figure 4 depicts CO_2 separation and capture technologies in a contemporary system. Modern CCU technologies abate CO_2 by absorbing air supply, isolating CO_2 (although in reduced concentration) and diluting it in N_2 and NOx molecules (post-combustion). The fundamental concept behind the pre-combustion approach is gasification, which occurs when carbonaceous biomass and coal are pyrolysed at high temperatures to form syngas, which results in the creation of H_2, CO and CO_2, particularly at high reaction temperatures (Valluri et al. 2022). The oxy-combustion technique burns fuel in recycled flue gas (RFG) with a proportion of oxygen rather than pure air (in conventional post-combustion). A considerable proportion of CO_2 gas and minute amounts of water vapour are produced; these gases are separated by adding a desiccant (such as SiO_2) that can absorb the moisture, yielding CO_2 with a purity of between 80 and 90% and O_2 with a purity of 95%, respectively. During the chemical looping process, an O_2 carrier transfers the necessary O_2 for combustion from the combustion air to the fuel, typically an oxidised metal. Alternating between the fluidised bed for air and the one for fuel is the oxygen carrier (metal oxide). After mixing with the fuel, the MeO produces water vapour and carbon monoxide as exhaust gas (Rajabloo et al. 2023).

The carbon cycle process has a significant impact on environmental, climate and energy production. Energy efficiency and carbon efficiency for the FT synthesis have respectively increased by 18.4% and 86.9% compared to conventional coal-liquid and by 15% and 100% for methanol production systems, based on the report of Chen (Chen et al. 2016). Another prime contributor to CO_2 emissions is the heat from fossil fuels, which accounts for 70% of the global electricity supply, around 50% of which is obtained from the combustion of coal (Chen et al. 2016).

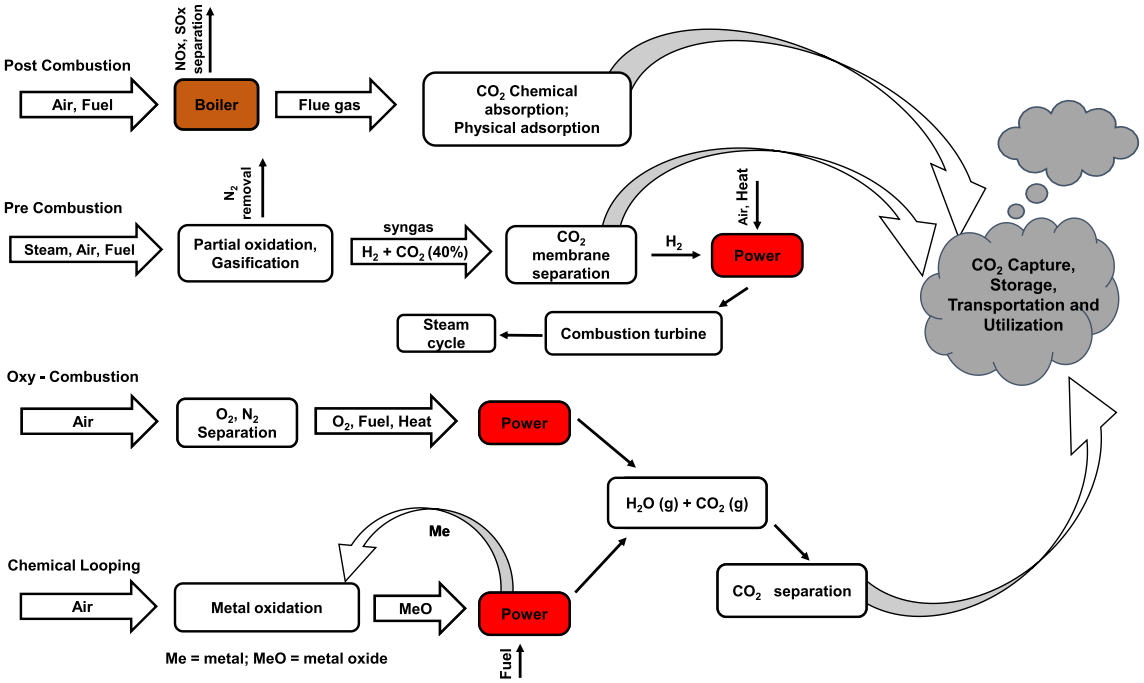

Fig. 4 Existing technologies for CO_2 capture and utilisation

Methane flaring and climate change

The world's energy consumption is thriving. The accomplishment of manufacturing civilisation, the expansion of the economy and the population's standard of living depend on energy usage. Consequently, the global energy consumption of all fuel sources has increased substantially. The usage of fossil sources (petroleum, coal and natural gas) is still dominant. It will continue to be essential soon, despite the year-by-year development of renewable energy sources (Sujianto 2020; Hatta et al. 2021). Global energy consumption, 1971–2019, displayed in Fig. 5a, highlights the six primary world energy sources, ranging from coal, oil, biofuels, hydro, natural gas and nuclear (This data is subject to the IEA's terms and conditions: https://www.iea.org/t_c/terms and conditions/. Natural gas is one of the most effective and considerable energy sources on the planet today. Due to its reliability and relatively high fuel economy, it remains an attractive option for the industrial and electric power sectors (Hatta et al. 2021). The worldwide usage of natural gas has increased during the previous two decades. According to (British Petroleum 2021, 2022), global natural gas consumption in 2021 was approximately 4.04 trillion cubic meters. The United States and Russian Federation are the most significant producers, accounting for almost 42% of the world's total natural gas, while in Fig. 5b, the various stages of raw biogas treatment to obtain clean biomethane are presented.

Although natural gas is an excellent fossil fuel and strategies to utilise the excess are ongoing, the scientific community agrees that anthropogenic greenhouse gas generation has consequently affected the global climate and that drastic reductions in these emissions are necessary to mitigate its adverse effects on climate change. Fossil fuel combustion, widely used for electricity, heat and transportation, is the primary source of emissions globally. Natural gas flaring releases approximately 300–400 million metric tonnes of CO_2 annually (Saidi 2018). The most common fossil fuels are coal, petroleum and natural gas. However, one common disposal method is flaring when there is inadequate infrastructure to use the gas locally, store it for energy, or transfer it via pipelines to market (Farniaei et al. 2014).

Most flared gas is CH_4, with minor amounts of volatile organic chemicals and inorganic molecules, such as CO_2, N_2 and water. There are two different types of gas flaring; associated flaring, which takes place in oil and gas (associated) reservoirs during exploration processes, and non-associated flaring, in which accumulated gas from refineries and petrochemical plants is flared for safety reasons, especially during normal routine operation. The volume and content of these gases vary depending on their production regions, as well as the temperature and pressure of the underground reservoirs from which they are extracted. Although no clear experimental data regarding the composition of the flared gas is available within our reach, in approximation, 80% of related gas flares are due to economic and technical constraints. According to a recent study by (Elvidge et al. 2015), upstream exploration and extraction facilities produce 90 % of flared gas globally. In recent years, extraction companies,

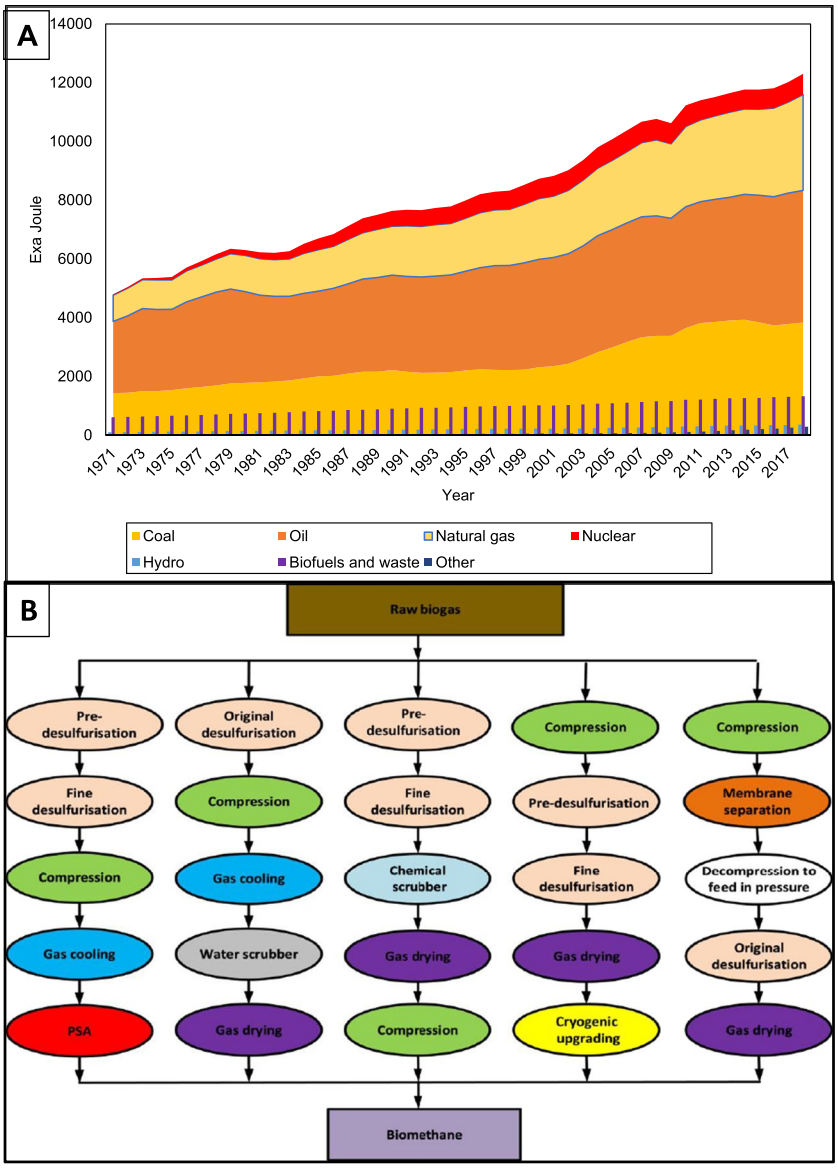

Fig. 5 **A** World total energy supply (by source), plotted based on data adapted from https://www.iea.org/t_c/termsandconditions/ with creative common's licence ("Key World Energy Statistics 2021"); **B** biogas cleaning/upgrading processes. Reused with permission from Rafiee et al. (2021)

pushed by environmental regulations and financial indications, have studied several options to reduce the quantity of flared gas. Collecting and transporting the gas to the market, converting it to a liquid fuel similar to gasoline, using it for electricity and heat generation, using it as a fuel for onsite needs, reinjection into underground strata to improve oil and gas extraction and the production of syngas are all methods for reducing gas flaring in addition to dry reforming processes (Orosa and Zardoya 2022; Tahmasebzadehbaie and Sayyaadi 2022; Owgi et al. 2023b), as summarised in Fig. 6. In a report published by (Fisher and Wooster 2019), gas flaring was mentioned amongst environmental catastrophes, potential global environmental crises and problems requiring attention.

Injection involves capturing flare gas emitted during flaring and reinjecting it into underground formations, such as depleted oil or gas reservoirs. This utilises the natural porous structure of the formations for storage. The technique allows for the storage of flare gas, which has the potential to reduce GHG emissions associated with flaring (Dinani et al. 2023). It also makes use of existing infrastructure, such as wells and pipelines. However, the effectiveness of injection depends on the geological characteristics of the storage formations. There may also be regulatory and operational challenges to overcome, such as obtaining permits and ensuring proper well integrity (Zayer Kabeh et al. 2023; Dinani et al. 2023). Despite these challenges, injection serves not only to mitigate emissions but also to enhance oil or gas recovery. It can be used in a variety of industries for emissions reduction and storage.

The gas to liquid/chemical (GTL/GTC) processes convert flare gas into liquid fuels or chemical products. This

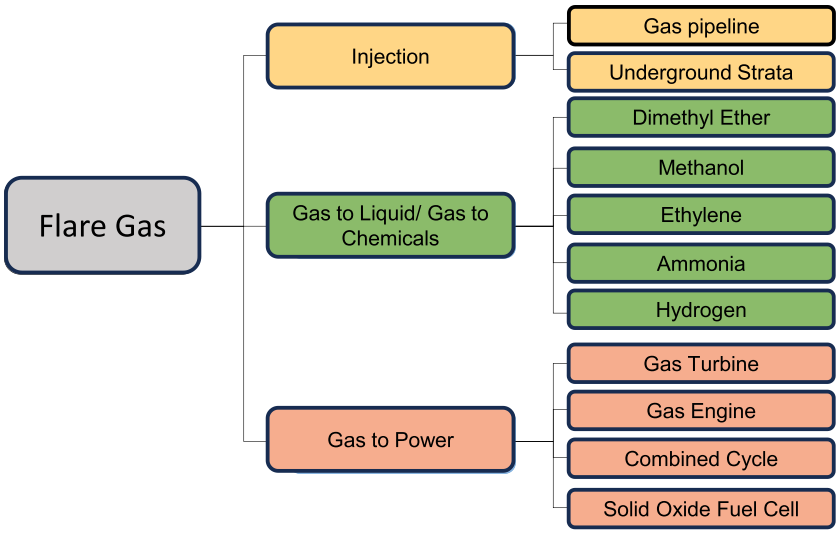

Fig. 6 Strategies for flare gas recovery and utilisation

is achieved through methods like FT synthesis or steam reforming. The processes yield valuable products, including DME, methanol, ethylene, ammonia and hydrogen. These technologies provide a way to monetise flare gas by producing higher-value products. They also offer alternatives to traditional fossil fuels and help diversify the energy mix (Orisaremi et al. 2023). However, GTL and GTC processes often require significant capital investment and complex infrastructure. They also have high energy and resource requirements, which can impact efficiency and the environmental footprint. Despite these challenges, GTL and GTC technologies offer solutions for emissions reduction and provide valuable products for various industrial applications (Dinani et al. 2023). They contribute to the transition towards sustainable energy systems.

Gas-to-power technologies efficiently convert flare gas into electricity using various methods, such as gas turbines, engines, combined cycle systems and solid oxide fuel cells (SOFCs). These technologies allow for the immediate utilisation of flare gas for onsite or grid-connected power generation (Orisaremi et al. 2023). While gas-to-power technologies can reduce flaring-related emissions and enhance energy efficiency, their deployment may require upfront investment in equipment and infrastructure. Additionally, efficiency and emissions performance can vary depending on the selected technology and operational conditions. Despite these challenges, gas-to-power technologies offer versatile solutions for using flare gas in various applications. This includes industrial operations, grid-connected power generation and off-grid power supply. They contribute to energy security and emissions reduction objectives (Orisaremi et al. 2023).

Strategies for mitigating methane prevalence

Generally, the strategies to modify methane reforming as the potential for mitigating pollution and energy generation have been in-depth, especially in recent years (Gao et al. 2018; Bahaghighat et al. 2019; Gao et al. 2021; Hatta et al. 2021; Yentekakis et al. 2021; He et al. 2022). The primary source from which methane is obtained is the associated and non-associated reservoirs (Muraza and Galadima 2015). As presented in Fig. 7, the most prevalent techniques range from the generation of synthetic gas from reforming such as auto-thermal, POX, dry and SR to other CH_4 and CO_2 conversion, utilisation and storage processes.

Dry reforming of methane (DRM)

The catalytic DRM (Eq. (1)) has attracted a lot of interest lately. This reaction produces syngas from two harmful greenhouse gases, CH_4 and CO_2. In addition to this benefit, the syngas is suitable for a variety of industrial processes, such as the production of higher hydrocarbons and oxygenated derivatives (such as methanol), because the molar ratio of H_2 to CO in the syngas is approximately equal to 1 (Radlik et al. 2015; Ibrahim et al. 2019; Kim et al. 2019).

$$CH_4 + CO_2 \rightarrow 2CO + 2H_2 \Delta H^0{}_{298\ K} = 247 kJmol^{-1} \quad (1)$$

The prime problems associated with DRM are excessive coke formation associated with the catalysts, the high temperature for the reaction and side reactions such as RWGSR (2), CH_4 cracking (3) and Boudouard reaction (BR) or CO disproportionation (4) (Schulz et al. 2015; Das et al. 2017; Bahari et al. 2021).

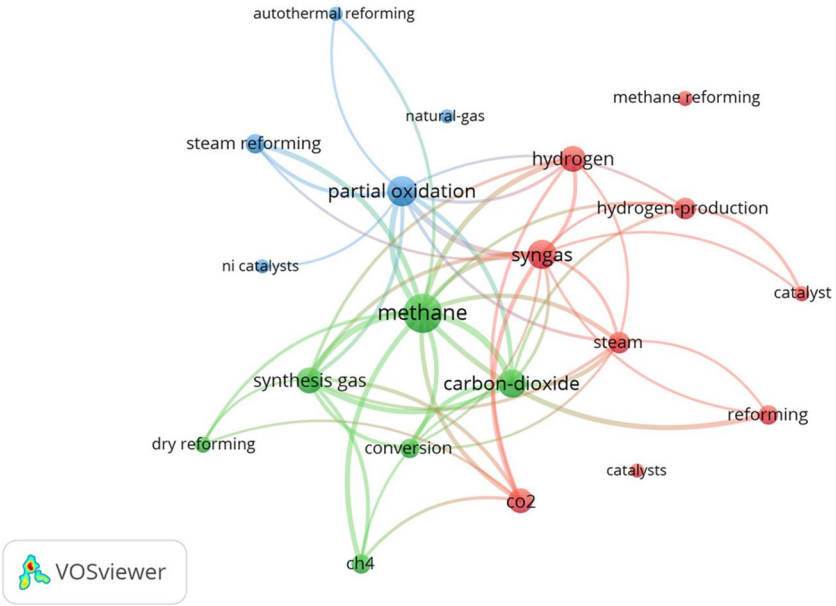

Fig. 7 Methane reforming perspectives. Generated using R-studio from plaintext file extracted from WoS

$$CO + H_2O \leftrightharpoons CO_2 + H_2 \qquad \Delta H^0{}_{298\ K} = -41.1\ kJmol^{-1} \tag{2}$$

$$CH_4 \leftrightharpoons C + 2H_2 \qquad \Delta H^0{}_{298\ K} = 75 kJmol^{-1} \tag{3}$$

$$2CO \leftrightharpoons C + CO_2 \qquad \Delta H^0{}_{298\ K} = -172 kJmol^{-1} \tag{4}$$

Equations (1) and (3) can favour the forward reaction by applying Le Chatelier's principle, increasing the reaction's temperature, removing the products as they form and introducing more moles of the reactants. In contrast, the reverse processes apply to Eqs. (2) and (4). Therefore, the RWGS and CO disproportionation prevail at low reaction temperatures, thereby depositing coke and generating CO_2.

Auto-thermal reforming (ATR)

The stand-alone technology capable of converting the entire methane in one reactor in the presence of fusion between exothermic POX and endothermic SR mechanisms is known as auto-thermal reforming (ATR). Catalytic ATR technology requires three critical reagents; CH_4, H_2O (steam) and air (O_2) to generate value-added syngas, as expressed in Eq. (5). This technology usually performs at a lower pressure than the POX process and has a low methane slip. The findings in the literature reported that the value of H_2/CO generated via catalytic ATR CH_4 is typically within the range of 1–2. Generally, the aim of combining POX and SR routes is to conserve energy since it does not require an external heat source. Indeed, catalytic ATR may boost the thermal conversion efficiency of H_2 generation and save operating expenses. However, the drawback of ATR CH_4 is the higher explosion risks due to the employment of oxygen as one of the necessary reactants. Besides, since this technology requires pure O_2, an expensive and complex O_2 separation unit must be installed in the system (Chong et al. 2019; Alhassan et al. 2023).

$$CH_4 + 0.25\ O_2 + 0.5\ H_2O \rightarrow \quad 2.5\ H_2 + CO \tag{5}$$

Like other CH_4 reforming processes, ideal catalyst selection contributes significantly to guaranteeing conversion and limiting coke accumulation during ATR since each type of catalyst can stimulate the reforming reaction through distinct pathways. Various catalysts in the literature have been used in ATR CH_4, including noble metal-based, non-noble metal-based and bimetallic catalysts (as summarised in Table 1). Li et al. compared the temperature profiles and the ATR performance of several noble metals (Pt, Rh and Pd) supported by spherical Al_2O_3 (Li et al. 2004). Amongst the employed systems, the Rh/Al2O3 catalyst demonstrated superior methane conversion (~ 100%) with a lower feed temperature than Pt and Pd-based catalysts. It was claimed that the metal particle distribution influenced the performance since the result of catalyst characterisation proved that Rh metal particles have better distributions, followed by Pt and Pd, in line with reforming activity. Indeed, the lower feed temperature exhibited by Rh/Al_2O_3 proved that the combustion reaction zone coincides with the reforming zone, which led to the heat transfer enrichment towards the endothermic section from the exothermic section.

In different studies, Ni et al. (2014) examined the impact of Ce-based oxides (Ce-LaO_x, Ce-GdO_x, Ce-SmO_x and Ce-ZrO_x) introduction over noble metal Rh supported with Al_2O_3 in CH_4 ATR. The authors also investigated the

Table 1 Summary of various catalyst systems utilised in CH_4 ATR

Catalyst	Synthesis	Conditions	Performance	Ref
Rh/Al_2O_3	IM*	T = 1123K W/F = 0.4 g h mol^{-1} P = 0.1 MPa $CH_4/H_2O/O_2/Ar$ = 20/10/20/50	X_{CH4} = ~ 100% H_2/CO = 2.3	(Li et al. 2004)
Pt/Al_2O_3			X_{CH4} = ~ 99% H_2/CO = 2.2	
Pd/Al_2O_3			X_{CH4} = ~ 78% H_2/CO = 0.8	
$Rh/Ce_{0.5}Zr_{0.5}O_2/Al_2O_3$	IWI*	T = 1003–1073 K GHSV = 20,000 h^{-1} $CH_4/H_2O/O_2$ = 1/2/0.46	X_{CH4} = 60–73%	(Ni et al. 2014)
Ni/SiO_2 (4.5 nm)	IM*	T = 973 K GHSV = 18,000 h^{-1}	X_{CH4} = 77.0% Cd = 12.9 mmol/gcat	(Hou et al. 2007)
Ni/SiO_2 (45.0 nm)			X_{CH4} = 47.2% Cd = 12.9 mmol/gcat	
NiCe/Al	WI*	T = 1123 K GHSV = 24,000 h^{-1} $CH_4/H_2O/O_2/Ar$ = 2/1/1/1	X_{CH4} = ~ 100% H_2/CO = 2.3 Cd = 0	(Kim et al. 2013)
$Ni/\alpha\text{-}Al_2O_3$	IWI*	T = 1023 K $CH_4/H_2O/O_2$ = 2/0.4/1	X_{CH4} = ~56.0–18.3 %	(Lisboa et al. 2011)
$Ni/Ce_{0.75}Zr_{0.25}O_2$			X_{CH4} = ~55.0%	
$Pt/\delta\text{-}Al_2O_3$	IWI*	T = 923 K $CH_4/H_2O/O_2/Ar$ = 2.12/6.36/1.0/5.36	X_{CH4} = ~ 46.6 %	(Karakaya et al. 2013)
$Pt\text{-}Rh/\delta\text{-}Al_2O_3$			X_{CH4} = ~ 51.2 %	
$NiPd/Ce_{0.5}Zr_{0.5}O_2/Al_2O_3$	SI*	T = 1023–1223 K $CH_4/H_2O/O_2/Ar$ = 1/1/0.75/2.5	X_{CH4} = 95.0% H_2/CO = 2.4	(Ismagilov et al. 2014)

IM impregnation, *WI* wet impregnation, *IWI* incipient wet impregnation, *SI* sequential impregnation

effectiveness of alkaline-earth metal oxides like K, Ca and Mg incorporation on the stability and coke resistance of Rh/Al_2O_3. The authors confirmed that the incorporation of Ce-ZrOx effectively lessens the CO generated during the reaction, resulting in a high H_2/CO ratio compared to other Ce-based oxides. Besides, keeping the atomic ratio between Ce and Zr nearly 1 to 1 was the ideal amount to improve the catalyst's thermal stability and catalytic activity efficiently. Alkaline-earth metal oxides were added, but no coke was deposited; yet, adding MgO showed a more stable performance than Rh-based catalysts combined with K and Ca metals.

Since precious metals are so costly and challenging, researchers have started looking into using cheaper, more abundant metals like nickel instead. On the other hand, nickel is frequently associated with deactivation due to coke deposition and sintering difficulties. The effect of Ni particle size on Ni-based catalyst deactivation in CH_4 ATR was examined by Shi et al. (2021). The researchers found that, in CH_4 ATR, smaller Ni-based catalyst particles were more active and stable than bigger ones, particularly at space velocities below 54,000 h^{-1}. They further clarified that the slower rate of side reaction (CH_4 decomposition) is responsible for coke deactivation compared to the rate of oxidative removal of surface carbons, causing the incomplete conversion of O_2. This phenomenon triggers Ni oxidation and leads to Ni deactivation.

Concerning deactivation matter, considerable effort has been made in the literature in modifying Ni-based catalysts for auto-thermal reforming CH_4. Kim and co-researchers (Kim et al. 2013) incorporated cerium oxide as the promoter for nickel-supported γ-alumina to tackle the deactivation and unstable issue due to coke accumulation. It was found that adding cerium oxide effectively enhanced the performance of the Ni-supported γ-alumina by recording ~ 100% of CH_4 conversion with no coke accumulation for 100-h reforming activity. The authors claimed that the $CeAlO_3$ phase formation within this catalyst structure accelerated the oxidation of coke and CO, affecting the catalytic stability and lowering CO selectivity. Indeed, an H_2/CO molar ratio of about 1.9 was generated from this process, lower than the typical ratio generated via POX and SR of CH_4 due to the unfavourable water-gas shift. In a different approach, Lisboa et al. (2011) employed Ni supported over $Ce\text{-}ZrO_2$ for the ATR of CH_4. The superior reforming activity (CH_4 conversion = ~ 55.0%) and stability compared to 10% $Ni/\alpha\text{-}Al_2O_3$ was achieved by $Ni/Ce_{0.75}Zr_{0.25}O_2$ within 25 h, assigned to the helpful between the metallic surface area and O_2 storage capacity and metallic surface area. It was noticed that O_2 generated during the dissociation of CO_2 assists in re-oxidise the support to stimulate a redox mechanism for continuous coke cleaning.

Besides developing monometallic catalysts, bimetallic catalysts have been successfully utilised in ATR CH4.

The impact of monometallic and bimetallic catalyst configurations using noble metals for the ATR of CH4 was compared by (Karakaya et al. 2013). Their work reported that the bimetallic Rh-Pt catalyst generated via incipient-to-wetness impregnation depicted an excellent conversion of CH_4 (31.0–51.2%) compared to monometallic catalysts (12.8–46.6%) regardless of reaction temperature (773–923 K). This trend resulted from the effective Pt-Rh interaction, which generated a synergetic effect that triggers higher conversion and reaction rates. A similar excellent catalytic performance of bimetallic catalysts was experienced by Ismagilov et al. using the Ni-Pd combination supported with $Ce_{0.5}Zr_{0.5}O_2/Al_2O_3$ via sequential impregnation technique (Ismagilov et al. 2014). Within the temperature range of 1023–1223 K, the authors reported an acquired 95% CH_4 conversion and ~ 75% H_2 yield attributed to the catalyst's reducibility and dispersion enhancement.

Partial oxidation (POX) of methane

Catalytic POX CH_4 (Eq. (6)) is another promising alternative for generating syngas from CH_4 for downstream process requirements. This route typically operates at a high temperature (1473–1773 K) in the absence of a catalyst and a moderate temperature (1023–1173 K) with catalysts, along with utilising a non-stoichiometric ratio of CH_4/O_2 as necessary reactants (Zhan et al. 2010; Velasco et al. 2014). Since this route is considered a mildly exothermic reaction, it offers a more economically feasible process as it consumes less energy than highly endothermic SR. Additionally, the synthesis gas generated via this technology typically consists of an H_2/CO ratio of 2, appropriate for downstream processes like FT and methanol synthesis without further adjustment. Remarkably, the generated undesired gases along this route also contain extremely low undesirable CO_2 compared to others, which must be eliminated before employing syngas in downstream reactions. Although the POX route offers advantages in terms of energy efficiency, the requirement of O_2 separation and desulphurisation units involves expensive operational costs, limiting this technology's extensive implementation for industrial applications (Elbadawi et al. 2021). Indeed, due to the rapid reaction steps, it is challenging to eliminate the heat generated within the system, which is risky and could even trigger explosions.

$$CH_4 + {}^1/_2\,O_2 \rightarrow CO + 2H_2 \qquad \Delta H^0{}_{298\ K} = 36 kJmol^{-1} \tag{6}$$

In 1929, Liander and co-researchers initiated the POXM for syngas production (Liander 1929). They claimed that high yields of syngas were only attained at temperatures around 1123 K, while non-equilibrium product distributions were acquired at a temperature lower than 1123 K. Since then, various catalysts, including supported noble and non-noble metal oxides as well as bimetallic catalysts, have been utilised for the catalytic methane POX. Table 2 summarises several common catalysts that have been used in the POXM.

Noble metals are known for their better performance in the catalytic oxidation of methane in terms of activity and resistance to coke formation. The performance of a range of noble catalysts supported by Al-Mg (Pt, Ir, Pd, Rh and Ru) synthesised via impregnation was evaluated by Khajenoori et al. (2013) for catalytic POXM at 973 K and CH_4/O_2 ratio of 2. Amongst the tested catalysts, Rh and Ru were found to be the most active, with about ~ 73–74.0% CH_4 conversion, close to the thermodynamic equilibrium values (76.3%) for the catalytic oxidation of CH_4, followed by Ir (72.1%), Pt (68.4%) and Pd (59.0%). This trend corresponded to the excellent metal distribution with a small crystallite size (5 nm) on the Al-Mg support. Additionally, the H_2/CO ratios for all the catalysts were obtained close to equilibrium levels (2.11), at about 1.8–1.9. However, because of the reverse water gas shift, the more significant value of H_2/CO (2.4–5.8) was obtained at low temperatures (923 K). Amazingly, none of the tested noble catalysts showed any signs of deactivation after 50 h of stable functioning. Ahn and co-workers also reported a similar outstanding performance on noble metals during the comparative evaluation of CeO_2-supported metallic catalysts (Pt, Ir, Pd, Ru, Ni and Rh), accredited to smaller particle size, excellent metal distribution and intense metal support interaction (Ahn et al. 2011). Nevertheless, the expensive cost and minimal reserves of these types of noble metals shifted the attention of researchers towards non-noble metals like Ni and Co, which are more attractive and practical for commercialisation.

Swaan et al. (1997) compared Ni- and Co-based catalysts for the POXM to syngas at 873–1173 K with a feeding ratio of $CH_4/O_2/He/N_2$ about 10/5/80/5. They found that Ni-based catalysts were superior in activity and selectivity in the POXM, although Co-based catalysts were very reactive for the combustion of CH_4 to CO_2. Since then, massive efforts on Ni-based catalyst development for POXM have been reported in the literature. Liu et al. evaluated the performances of Ni-supported catalysts by distinct alumina species, including α-Al_2O_3, γ-Al_2O_3 and θ-Al_2O_3, in the POXM (Liu et al. 2002). It was evidenced that Ni supported on γ-Al_2O_3 exhibited superior CH_4 conversion ~ 89.0% and stable within 24 h compared to Ni/θ-Al_2O_3 (~ 86.2%) and Ni/α-Al_2O_3 (~ 78.3%), owing to the inferior size of Ni particles (7.8 nm) and vast surface area (191 $m^2\ g^{-1}$). The high CH_4 conversion (90.5–94.7%) and CO selectivity (93.9–96.8%) were also experienced by Lu et al. during the employment of Ni/γ-Al_2O_3 catalysts, regardless of reduction temperature (873–973 K) and GHSV of (612–1152 L g^{-1} h^{-1}) (Lu et al. 1998).

Table 2 Summary of catalysts reported for the partial oxidation of methane

Catalyst	Synthesis	Conditions	Performance	Ref
Pt/Al-Mg	IM*	T = 973 K GHSV = 16,000 ml h^{-1} g_{cat}^{-1} CH_4/O_2 = 1/2	X_{CH4} = 68.4% H_2/CO = 1.93	(Khajenoori et al. 2013)
Ir/Al-Mg			X_{CH4} = 72.1% H_2/CO = 1.86	
Rh/Al-Mg			X_{CH4} = 74.1% H_2/CO = 1.89	
Ru/Al-Mg			X_{CH4} = 73.1% H_2/CO = 1.92	
Pd/Al-Mg			X_{CH4} = 59.0% H_2/CO = 1.94	
Ir/CeO_2	IM*	T = 1023 K CH_4/O_2/He = 2/1/10	X_{CH4} = 97.0% H_2/CO = ~ 2	(Ahn et al. 2011)
Ru/CeO_2			X_{CH4} = 96.2% H_2/CO = ~ 2	
Pd/CeO_2			X_{CH4} = 90.2% H_2/CO = ~ 2	
Ni/CeO_2			X_{CH4} = 99.1% H_2/CO = ~ 2	
Pt/CeO_2			X_{CH4} = 93.2% H_2/CO = ~ 2	
Rh/CeO_2			X_{CH4} = 84.6% H_2/CO = ~ 2	
Ni/α-Al_2O_3	IM*	T = 1018–1033 K GHSV = 27,600 ml h^{-1} g_{cat}^{-1} CH_4/O_2 = 1.95/1	X_{CH4} = ~ 78.3% S_{CO} = 89.1%	(Liu et al. 2002)
Ni/γ-Al_2O_3			X_{CH4} = 89.0% S_{CO} = 95.3%	
Ni/θ-Al_2O_3			X_{CH4} = 86.2% S_{CO} = 95.2%	
Ni/γ-Al_2O_3	IM*	T = 873 K GHSV = 612–1152 l h^{-1} g_{cat}^{-1} CH_4/O_2 = 2/1	X_{CH4} = 90.5–94.7% S_{CO} = 93.9–96.8% S_H = 97.8–99.0% H_2/CO = 2.04–2.08	(Lu et al. 1998)
Ni-Al	PH*	T = 973 K CH_4/O_2 = 2/1 TOS = 20 h	X_{CH4} = 73.4%	(Kim et al. 2004)
Ni-IMP	IM*		X_{CH4} = 67.3%	
Tr-Ni	PCP*	T = 1023 K CH_4/O_2 = 2/1 TOS = 6 h	X_{CH4} = 46.3% Y_{CO} = 0.79 mol	(Lucrédio et al. 2007)
Ae-LaNi	AE*		X_{CH4} = 43.7% Y_{CO} = 0.95	
Ae-CeNi			X_{CH4} = 48.1% Y_{CO} = 0.92	
Ni/SBA-16	IM*	T = 1023 K GHSV = 18,000 ml h^{-1} g_{cat}^{-1} CH_4/O_2 = 2/1	X_{CH4} = 92.0% H_2/CO = 1.51	(Shokoohi Shooli et al. 2018)
Cu-Ni/SBA-16			X_{CH4} = 89.8% H_2/CO =1.49	
Ce-Ni//SBA-16			X_{CH4} = 93.0% H_2/CO =1.66	
Ni/SBA-15	IM*	T = 1023 K GHSV = 18,000 ml h^{-1} g_{cat}^{-1} CH_4/O_2 = 1.9/1	X_{CH4} = 92.0% S_{CO} = 94.6% S_H = 95.0%	(Habimana et al. 2009)
Ni/Cu/SBA-15	SI*		X_{CH4} = 95.0% S_{CO} = 94.1% S_H = 97.2%	

Table 2 (continued)

Catalyst	Synthesis	Conditions	Performance	Ref
Ni/MgO-Al_2O_3	ICIM*	T = 1073 K GHSV = 80,000 h^{-1} CH_4/O_2 = 1.9/1	X_{CH4} = 5.6% S_{CO} = 55.3% S_H = 50.0%	(Qiu et al. 2007)
NiCeCa/MgO-Al_2O_3			X_{CH4} = 75.1% S_{CO} = 82.1% S_H = 85.0%	
Ni/γ-Al_2O_3	IM*	CH_4/O_2 = 2/1	X_{CH4} = 78.2% S_{CO} = 93.5%	(Wang et al. 2004)
Ni/La_2O_3/γ-Al_2O_3			X_{CH4} = 80.2% S_{CO} = 94.8%	
Ni/CaO/γ-Al_2O_3			X_{CH4} = 77.9% S_{CO} = 92.7%	
Ni/CeO_2/γ-Al_2O_3			X_{CH4} = 80.3% S_{CO} = 95.4%	
Ni/γ-Al_2O_3	IM*	T = 873-973 K CH_4/O_2 = 2/1	X_{CH4} = 28.2% Y_{CO} = 15.7% Y_H = 15.3%	(Cheephat et al. 2018)
Re/γ-Al_2O_3			X_{CH4} = 6.7% Y_{CO} = 1.1% Y_H = 2.5%	
Re-Ni/γ-Al_2O_3			X_{CH4} = 100% Y_{CO} = 87.4% Y_H = 92.8%	
Ni/CeO_2	BM*	T = 823 K GHSV = 12,000 h^{-1} CH_4/O_2 = 1.73/1	X_{CH4} = 22.0% S_{CO} = 0% S_H = 0%	(Fazlikeshteli et al. 2021)
Pd–Ni/CeO_2			X_{CH4} = 71.8% S_{CO} = 21.7% S_H = 65.5%	
Ni/ZnO-NPr	WI*	T = 1123 K CH_4/O_2 = 2/1	X_{CH4} = 92.7% S_{CO} = 23.0% S_H = 44.8%	(Javed et al. 2021)
Ni-Co/ZnO-NPr			X_{CH4} = 98.0% S_{CO} = 22.1% S_H = 42.3%	

Sco,$S_{H,}$ = selectivity of CO and H_2 respectively; Yco, Y_H= yield of CO and H_2 respectively; XCH_4 = conversion of CH_4; *BM* ball milling, *WI* wet impregnation, *PH* post-hydrolysis, *PCP* precipitation, *AE* anionic exchange, *SI* sequential impregnation, *ICI* incipient impregnation, *PCP* precipitation

Although Ni-based catalysts demonstrated comparable activities with noble metals, this material is known for their sintering and coke issues which contribute to deactivation. Several approaches have been implemented to overcome these drawbacks, ranging from support selection and modification to incorporating second metals as promoters or forming bimetallic catalysts. Mesoporous alumina synthesised via the post-hydrolysis method, according to Kim et al., improved Ni activity and lowered the coke accumulation during POXM (Kim et al. 2004). The authors stated that the incorporation of mesoporous alumina with Ni (Ni/Al ratio 1:10) led to intense Ni-Al interaction, causing the excellent distribution of Ni particles. Indeed, the relatively huge surface area (282.4 m^2 g^{-1}) and pore volume (0.26 cm^3 g^{-1}) with a narrow pore size distribution (3.3 nm) explained the superior activity (73.4%) and were more resilient to coke accumulation than the Ni catalyst impregnated on commercial alumina (Ni-IMP) during 20 h of reaction.

Lucrédio and colleagues tackled the coking nature of Ni-based catalysts in POXM by introducing lanthanum and cerium via the anion exchange technique (Lucrédio et al. 2007). It was noticed that interaction between Ni supports was considerably improved after both promoters' incorporation, attributed to enhancements in Ni active species distribution on the support surface. Although there was no significant improvement in CH_4 conversion after incorporating lanthanum and cerium, the authors observed stable conversion activity with enrichment in CO yield within 6 h on the stream. The authors justified that adding those promoters favoured the adsorption and decomposition of O_2 on

the catalyst's surface, thus assisting the carbon gasification process. Similar findings were reported in the literature with the incorporation of various kinds of promoters, including Cu (Habimana et al. 2009; Shokoohi Shooli et al. 2018), Ca (Qiu et al. 2007; Habimana et al. 2009) and Mg (Ma et al. 2019).

Besides monometallic catalysts, several series of bimetallic commonly consisting of Ni-based have been widely utilised in the POXM since these combinations can improve catalytic activity, stability, selectivity and coke resistance. Cheephat et al. (2018) synthesised Re-Ni bimetallic catalyst via impregnation and tested it in POX within 673–973 K (Cheephat et al. 2018). The authors found that Re-Ni bimetallic catalyst with a Re:Ni ratio of 3:7 depicted superior CH_4 conversion (~ 100) and product yields (CO = 92.8 %, H_2 = 87.4%) at temperature 973 K compared to monometallic Ni/γ-Al_2O_3 and Re/γ-Al_2O_3. Bimetallic catalysts did exhibit remarkable catalytic stability with a very small deactivation of H_2 production (7.4%), whereas monometallic Ni/γ-Al_2O_3 and Re/γ-Al_2O_3 experienced enormous catalyst deactivation of about 63.9% and 19.1%, respectively. This more excellent outcome was attributed to a better distribution of Ni after combining with Re species. Fazlikeshteli et al. (2021) and Javed et al. (2021) also reported comparable findings after forming bimetallic catalysts between Co-Ni and Pd-Ni species. Both authors justified that the bimetallic combination approach effectively improved the dispersion metal and metal support interaction, causing the increment in the accessible active site and coke resistance, thus, leading to excellent catalytic activity and stability.

Steam reforming of methane (SRM)

The first attempt to investigate the reaction between CH_4 and steam in the industry was done and published by Neumann and Jacob in 1924 (Ighalo and Amama 2024). SRM is concerned with the thermo-catalytic transformation of natural gas (mainly CH_4) into syngas and pure H_2. This material is a valuable feedstock for a variety of high-value petrochemicals. However, due to its high heating value of roughly 140 kJ/g and the creation of carbon-free H_2, it appears to be an appealing energy option and hence a critical starting point in the emerging H_2 economy (Ali et al. 2023). The SRM involves three bidirectional reactions depicted above in Eqs. (2), (7) and (8), respectively. Two of the reactions (Eqs. (7) and (8) are endothermic, whereas the water gas shift process (Eq. (2)) is exothermic (Guo et al. 2012; Seelam 2013; Boretti and Dorrington 2013). Conditions of reactions, steam-to-methane ratio and important findings from related works in steam reforming (SR) are presented in Table 3.

$$CH_4 + H_2O \leftrightharpoons CO + 3H_2 \qquad \Delta H^0{}_{298\ K} = +206 kJmol^{-1} \tag{7}$$

$$CH_4 + 2H_2O \leftrightharpoons CO_2 + 4H_2 \qquad \Delta H^0{}_{298\ K} = +165 kJmol^{-1} \tag{8}$$

Catalyst deactivation occurs majorly by coke formation due to CH_4 cracking (Eq. (3)) and the BR, also known as the CO disproportionation (Eq. (4)).

Photothermal Reforming (PTRM)

Solar energy could replace fossil fuels well because it is clean, widespread and never runs out. The notion of photothermal catalysis and its use in DRM processes was recently published. In line with the literature, photothermal catalytic DRM may significantly increase syngas production compared to a single thermal condition by combining infrared light's thermal action with ultraviolet light's photoelectric impact. For the above reasons, photothermal catalysis is developing into a competitive and promising technology. Based on publicly available research studies, Ni-based photothermal catalysts have high DRM catalytic activity (Zhong et al. 2022). Solar energy can be used to electrify, fuel, heat and cool buildings using photovoltaics, concentrated solar heating/power, photo/thermal chemical conversion and so on (Chen et al. 2022; Zheng et al. 2022). Amongst the different solar-to-chemical conversion technologies, solar-to-chemical conversion is both challenging and intriguing since it can alleviate two contemporary human problems: the energy crisis and environmental pollution. Since CO_2 and CH_4 are both greenhouse gases and relatively stable (C—O bond energy is 750 kJ/mol, C–H bond energy is 430 kJ/mol), solar-powered DRM would yield syngas, which can be easily recycled, more energy-saving with reduced emissions and enhanced storage potential.

Zhang et al. (2019) and Araiza et al. (2021) conducted in situ diffuse reflectance infrared Fourier transform spectroscopy (DRIFTS) at various temperatures with and without light irradiation to gain a better knowledge of the thermal influence on energetic hot carriers (EHC) (Fig. 8). At the furnace temperature of 150 °C, no indication of DRM initiation can be seen in the absence of light irradiation. The presence of HCO_3 indicates that both CO_2 and CH_4 were activated in the presence of light (1685/1420 cm^{-1}), CO_3^{2-} (1557 cm^{-1}), COOH (1653 cm^{-1}) and CHX (2824/1440 cm^{-1}) species. This demonstrates unequivocally that the EHC may surmount the DRM thermodynamic barrier. The EHC uses two routes in photocatalytic DRM: (i) converting CO_2 to CO right away with CO_2^- as an intermediate; (ii) reducing CO_3^{2-} to COOH as an intermediate and subsequently to CO. In the second process, water can be produced as a by-product. The majority of EHCs opt to choose the second route, which lowers the H_2/CO ratio because there

Table 3 Reported conditions for steam reforming of methane in recent literature

Catalyst system	Conditions	Findings	Ref
Y-promoted Ni-based catalyst, supported over Al_2O_3	600, 650, 700 °C; S/M ratio 1.5, 2.5 and 3.5; Ni loadings 0,1.5 and 3wt %; Y loadings 0, 1.5 and 3wt %	Outperforming system was 16.2Ni-2.7Y/HS-Al at 690 °C and S/M ratio 3.4; CH_4 conversion 93.8%; H_2 yield 97.4 %.	(Salahi et al. 2023a)
Y-promoted Ni-based catalyst, supported over hollow Al_2O_3	600, 650 and 700 °C; S/M ratio 1.5 to 3.0; Ni loading 15, 20 and 25wt %; Y loading 1.5, 3 and 4.5wt %	20Ni-3.0Y/HAl showed highest CH_4 conversion and H_2 yield of 95.77% and 97.74 %, respectively; H_2/CO molar ratio of 6.61 at 700 °C.	(Salahi et al. 2023b)
InnovaTek Catalyst; 12Ni/Al_2O_3	800 °C, S/M ratio 3.6, iso-octane, natural gas, retail gasoline and hexadecane	InnovaTek displayed outstanding activity @ CO concentration to < 1 % by WGS reaction; the sulfur tolerance @220h using iso-octane with 100 ppm sulfur.	(Ming et al. 2002)
Ni/Ce-ZrO_2 and Ni/YSZ	Methane, methanol and ethanol reforming at 900 °C with the inlet fuel/steam molar ratio of 1.0/3.0 (partial pressure of inlet feed of 4 kPa).	To determine the stability and deactivation rate, the reforming rate was calculated as a function of time.	(Laosiripojana and Assabumrungrat 2007)
Ni/SiO_2	600, 700 and 800 °C, S/M ratio of 0.5	Plasma-prepared catalysts averaged 5.5 nm, compared to 15.3 nm for thermally calcined ones; smaller catalysts can resist coke better than plasma-prepared catalysts; plasma-prepared catalysts display different carbon nanotubes than calcined catalysts.	(Zhang et al. 2015)
Ni-dispersed TiO_2-$ZnTiO_3$ perovskite	5/95–15/85wt % phenol/water feed concentration; 20 ml min^{-1} of N_2; feed flow rate 10–30 ml h^{-1}; loading of catalyst 0.2–0.4 g; 600–800 °C; 1 atm.	TiO_2-$ZnTiO_3$ had enhanced Ni dispersion, H_2 yield and phenol conversion; Ni/TiO_2-$ZnTiO_3$ had better stability than Ni/TiO_2 nanoparticles.	(Baamran and Tahir 2019)
Reducible tri-metallic NiO/TiO_2/Co_3O_4 nanocubes	700 °C; 0.3 g catalyst, and 5% phenol feed concentration.	Strong metal interaction with reducible support minimised coking; prolonged stability was recorded for Ni/TiO_2-Co_3O_4 than Ni-Co/TiO_2 nanoparticles.	(Abbas and Tahir 2021)
Rh supported over MgO, CeO_2, ZrO_2 and mixed metal oxides Mg–Ce–O, Mg–Zr–O and Mg–Ce–Zr–O	575–730 °C; 0.3 g catalyst total gas flow rate 200 N ml/min	When compared to a commercial Ni-based tar SR catalyst, the 0.5wt% Rh/MgO and 0.1wt % Rh/Mg-Ce-Zr-O catalysts with sol-gel supports performed better.	(Polychronopoulou et al. 2004)
Ni-Co/ZrO_2	0.2 g catalyst diluted by 0.3 g silicon carbide; steam-phenol preheater temperature of 200 °C; 30 ml/min N_2 as diluent; phenol - steam flow was 1:9 mol/mol	The catalyst prepared by the hydrothermal method was uniform and did not agglomerate; catalytic reforming of Polyethylene terephthalate produced numerous branched chains aliphatics.	(Nabgan et al. 2019)
Mg-modified Ni/Attapulgite (ATP)	800 °C; flow of H_2/N_2 at 0.1 L/min.	The production of amorphous coke and the sintering of nickel grains are inhibited by Mg-modified Ni/ATP.	(Qingli et al. 2021)

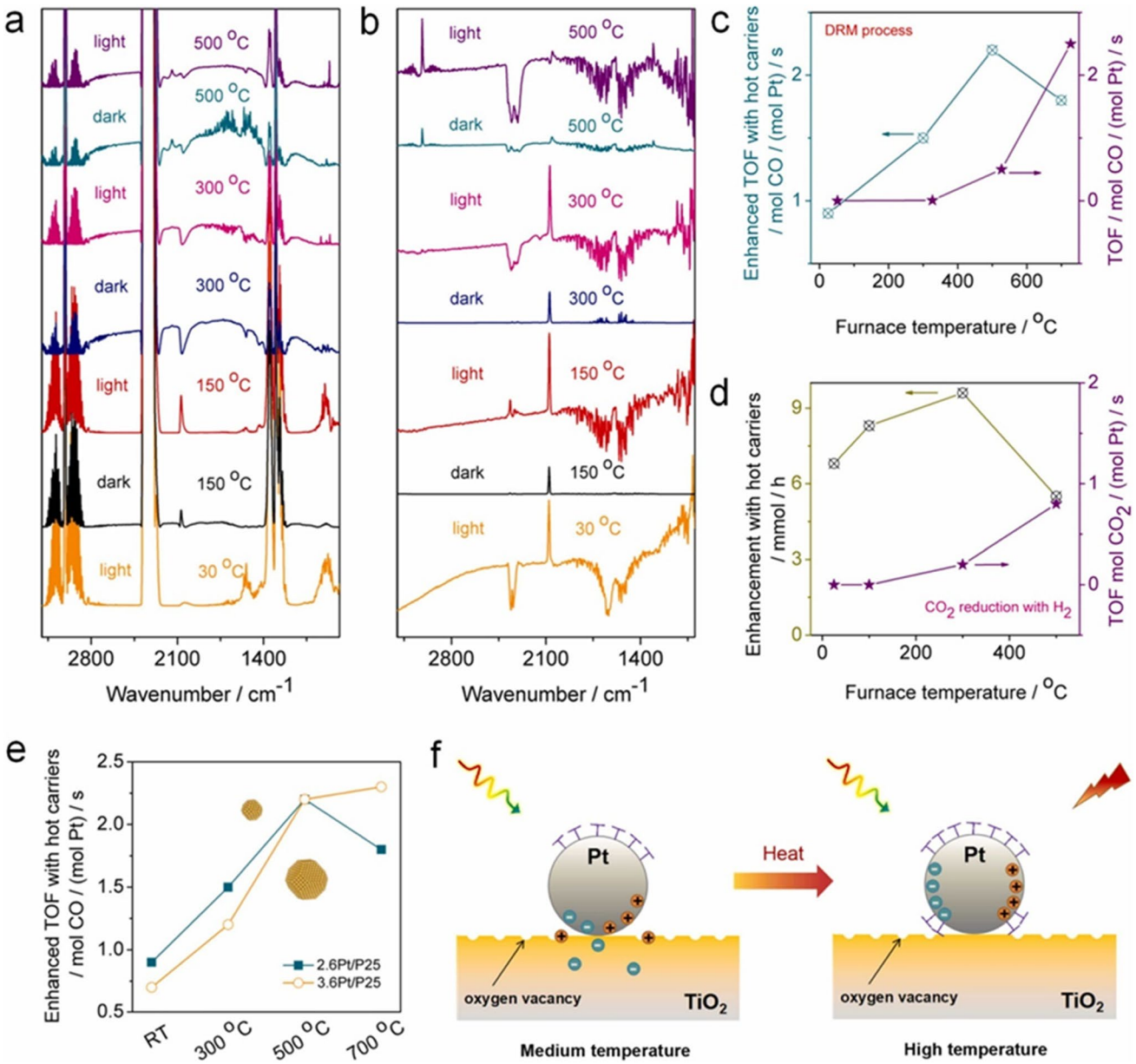

Fig. 8 In situ DRIFTS spectra with and without illumination for **a** DRM and **b** CO_2 reduction with H_2. **c** Improved TOF with EHC and thermally assisted TOF at varying temperatures in DRM. **d** Increased electron transfer with EHC and thermally assisted TOF at different temperatures in the CO_2 reduction process. **e** Improved TOF with EHC at varying temperatures on P25-supported Pt NPs of varying sizes, and **f** a schematic of the thermal suppress effect on EHC (adapted with copyright permission from (Zhang et al. 2022a))

are fewer EHCs at normal temperatures that have the energy to overcome the higher redox potentials of reactants. When the temperature is increased to 150 ⁻C in photothermal catalytic DRM, the CO_2 peak becomes stronger. In contrast, the peaks of other intermediates in the second pathway weaken, indicating that the two routes are augmented by increased photo-induced EHC and decreased CO_2/CO reduction potential, resulting in an elevated H_2/CO ratio.

Heterogeneous dissociation of CH_4 in the presence of a photocatalyst might occur due to the presence of a local electric field. The catalyst's ability to transport electrons is most likely a critical factor in the activation of CH_4 and the formation of methyl radicals (He et al. 2022). As a result, lowering the activation energy barrier effectively may be accomplished by CH_4 catalytic conversion. Therefore, developing more cost-effective and effective CH_4 utilisation methods with catalyst support is extremely important. During the light-off operation, the temperature decreased quickly, stabilising the heat release and dissipating the photothermal storage capacity of ATR@PCM and ATF@PCM, which first

Table 4 Abridged novelties in photothermal catalysts for methane conversion

Photo/thermal catalyst	Loading/ratio/intensity	Temperature, flow rate	Findings	Ref
Ti@TiO_2 photocatalyst	7.8 mg of photocatalyst, 65 ml of aqueous glycerol; ozone-blocking ASB-XE-175W xenon lamp. X1-1 Optometer detected light power 8 cm from the reactor.	Temperature of mixture, 95 °C. A volumetric flow metre regulated the Ar gas flow at 58 ml min^{-1}	100–150 °C crystallises Ti (IV) amorphous species and oxidises Ti_3O on TiO nanoparticles to form TiO_2 NPs; Overheated water oxidises TiO_2 at 150 °C; kinetic studies and electrochemical impedance spectroscopy demonstrate higher electron transport in Ti@TiO_2 nanoparticles; Ea = 25–31 kJ mol^{-1} suggests photothermal influence from glycerol oxidation intermediate diffusion or water dynamics at the catalyst surface	(El Hakim et al. 2021)
Pt/TiO_2		Prior to the reaction temperature, the catalyst was activated by H_2 for 1h at 700 °C with a flow rate of 20 ml/min.	Photo-induced EHC without external thermal energy provides most of the reaction rate, but thermo-catalytic outputs at the same external furnace temperature with photothermal catalysis (room temperature) are slow	(Zhang et al. 2022a)
2D Au/TiO_2 nanoflakes	50 mg catalyst; NR; 300-W Xe arc lamp	Temperature 25 °C, NR	Photothermal glycerol reforming requires photo-generated carriers; plasma-excited electrons Au nanoparticles did not directly or indirectly contribute to hydrogen generation; Hot carriers thermalised reactants, promoting intermolecular collisions	(Zhong et al. 2022)
Ni/mesoporous TiO_2 photothermal catalyst	The 0.2 g catalyst is purged with feed gas at a flow rate of 48 ml min^{-1}, with a ratio of CH_4, CO_2 and N_2 of 10:14:24; different light intensities (1.85 W/m^2, 2.45 W/m^2, 3.1 W/m^2) and spectral ranges (200–400 nm, visible-near-infrared light.	Mesoporous TiO_2 was evaluated at 500 °C, while Ni/mesoporous TiO_2 was tested at 550 °C and 600 °C.	The study tests a Ni/mesoporous TiO_2 composite catalyst for methane dry reforming. Results show strong CH_4/CO_2 conversion and CO/H_2 selectivity improvements. Mesoporous TiO_2 and Ni active sites synergistically improve catalytic performance under different lighting conditions. This study suggests using photothermal synergies to boost photochemical conversion.	(Xie et al. 2022)
(Ni/CeO_2)@SiO_2 catalyst	5–20 mg catalyst; Xe light (CEL-HXF300, 300 W Xenon lamp with radiant output of 50 W and spectral output of 300–2500 nm).	873 K under N_2, Next, $CH_4/CO_2/N_2$ (molar ratio of 3/3/4, 50 ml/min) was introduced into the reactor at GHSV of 120–600 L/(gcath)	The (Ni/CeO_2)@SiO_2 catalyst exhibits size effects, Ni-ceria interaction, confinement effect and significant visible solar light adsorption due to ceria's small band gap energy. CH_4 and CO_2 activations and CHx gasification improved with adsorption.	(Han et al. 2021)

Table 4 (continued)

Photo/thermal catalyst	Loading/ratio/intensity	Temperature, flow rate	Findings	Ref
$Ru/SrTiO_3$	The quartz reaction tube received 150 mg catalyst; under 300-W xenon lamp irradiation	36:36:28 CH_4:CO_2:N_2 input gas. With a total flow of 45 ml min^{-1}, the GHSV of 4592 h^{-1}; 0.1 MPa and 200–600 °C temperatures.	Light-induced charge transfer improves catalytic activity and stability. Charge transfer from $SrTiO_3$ to Ru lowers energy barriers for CH_4 dissociation and H_2 production, enhancing catalytic activity, H_2/CO ratio and RWGS suppression. The study improves photothermal DRM mechanism comprehension and solar photothermal greenhouse gas conversion	(Tang et al. 2023)
Pt-Au/P25 photothermal catalyst (Pt-Au/P25, Au/P25, Pt/P25 and P25)	0.05 g prepared catalyst, mixed with 0.1 g quartz sand; Xenon light, XE-300	50 vol% CO_2, 50 vol% CH_4, total flow rate of 20 ml min^{-1}	The Pt-Au/P25 catalyst yielded 201.92 and 85.38 mmol/g_cat/h CO and H_2 at 500 °C, 2.08 and 3.09 times higher than in dark circumstances. Well-distributed active sites and light responsiveness support this performance, according to SEM, TEM and UV–vis–NIR spectroscopy. Loading-induced defect sites and Au nanoparticle surface plasmon resonance effect enhance spectrum responsiveness, especially in the UV and around 565 nm	(Zhang et al. 2022b)
Cu/CeO_2 catalysts	50 mg Cu/CeO_2 catalysts, reduced by 20% H_2/N_2 at 300 °C for 30 min, Xenon lamp (Microsolar 300)	GHSV of 18 L/(gcath). Temperature 150 to 300 °C, CH_3OH/H_2O mixture with molar ratio of 1:1	Three Cu/CeO_2 catalysts with different Cu concentrations were synthesised for sustainable hydrogen production. The 10%-Cu/CeO_2 composite absorbed the lightest and interacted well with metal. Optimised catalyst performance improved with light irradiation, achieving 95.5% methanol conversion and 36 ml/(gcatmin) H_2 yield at 250 °C. A good plasmonic catalyst design for photothermal reforming is applicable to other photo-sensitive catalytic processes	(Zhao et al. 2023)

Table 4 (continued)

Photo/thermal catalyst	Loading/ratio/intensity	Temperature, flow rate	Findings	Ref
Nanoscale Ni/CeO_2 catalyst	300-W Xenon lamp, catalyst mass not reported, the reduction gas (90% N_2 and 10% H_2) is kept for 2h at 700 °C to fully reduce the catalyst to Ni/CeO_2	10.3 ml min^{-1} for 2 h, temperature 400 °C or 600 °C, 29.1/32.0/38.9 vol% $CH_4/CO_2/N_2$	Photothermal (PTDRM) converts 39.74% more CH_4 than standard DRM at 45 °C lower temperature, according to the study. Light increases CH_4 dissociation and H_2 generation by migrating photo-generated carriers to the catalyst surface, lowering activation energy. Experiments show that light increases CH_4 conversion and H_2 generation	(Yan et al. 2023)
SiO_2 shell encapsulating Ni loaded on the CeO_2–ZrO_2 support	300-W xenon parallel light source (CEL-HXF300), temperature range of thermal/photothermal catalysis was 400–600 °C 50 mg catalyst	The argon flow rate was set to zero, instead, the inlet flow rate of CO_2 and CH_4 was controlled at a constant rate of 5 ml/min by a mass flow controller. variable GHSV of 12,000 ml g^{-1} h^{-1}, and 24,000 ml g^{-1} h^{-1}.	In normal and photothermal steam reforming, core-shell Ni/CeO_2–ZrO_2@SiO_2 catalysts were examined. The core-shell catalyst outperformed Ni/ZrO_2 and Ni/CeO_2 in both reactions. The Ni/CeO_2–ZrO_2@SiO_2 catalyst had the maximum photothermal CO_2 and CH_4 conversions and yields at 600 °C. Thermal stability and carbon buildup resistance was excellent after 60 h of continuous operation. Lower photothermal catalyst activation energies for CH_4 and CO_2 were observed. The catalyst's turnover frequencies (TOFs) increased dramatically in photothermal steam reforming, proving that light increases performance	(Tengfei et al. 2024)

Table 5 Catalysts systems utilised for combined reforming of methane

Catalyst	Preparation method	Metal wt. %	Conditions	Conversions (%)		Ref
				CO_2	CH_4	
Ni-Mg(Ca)-Al_2O_3	Evaporation-induced self-assembly (EISA) method	Ni-x % (x: 5–10 wt %); and Ni5 %M5% (M: Ca or Mg)	800 °C, 1 atm, GHSV = 138Lgcat^{-1} h^{-1}	80	84	(Jabbour et al. 2017)
Ni/Al_2O_3, Ni/MgO-Al_2O_3, Ni/La_2O_3-Al_2O_3	Refluxed co-precipitation method and impregnation method	10wt. %	600, 650, 700 °C; 0.5g cat, CH_4:CO_2:H_2O:Ar 1:0.5:0.8:5.2	70	80	(Dan et al. 2021)
Biochar, Ni, Fe and K over Biochar	Microwave-assisted pyrolysis, followed by mechanical mixing	1:9 metal to biochar ratio, 10wt % metal loading, biochar particle size 0.23 to 0.35	700–900 °C, CO_2:CH_4:H_2O 30:30:60	77.8	82	(Li et al. 2019)
NiCe/MgAlSi for oxy-steam reforming	Sol-gel method, followed by incipient wetness impregnation	Si/Al ratio (0–5)	600, 700 and 800 °C; GHSV of 45,000 ml gcat^{-1} h^{-1} molar feed ratio CH_4:CO_2:O_2:H_2O = 1:0.67:0.1:0.3; atmospheric pressure.	80.4	91.7	(Doğan Özcan and Akın 2023)
Ce-promoted Ni/SiO_2 catalyst	Conventional co-impregnation	Ce/Ni molar ratios of NiCe-x/SiO_2 (x = 0.17, 0.50, 0.67, 0.84) catalysts	850 °C feed ratio CH_4:CO_2:O_2 = 40:20:10 total flow rate of 46.7 ml/min	76	88	(Li et al. 2013)
Biomass-derived biochar	Microwave-assisted pyrolysis, washing and drying	20 g of biochar average size of 0.33–0.83 mm soaked in 500 ml of solution	600–1000 °C, total gas flow of 300 ml·min^{-1} and 9 g of biochar	78.2	96.5	(Li et al. 2018)

Table 6 Outcomes and confrontation of the various reforming equations

Reforming equations	Description/challenges	Ref
SRM $CH_4 + H_2O \rightarrow 3H_2 + CO$	Ideal syngas ratio for FT long-chain hydrocarbons; less coke formation compared to other reforming processes; product ratio easily controlled by maintaining optimum steam to methane ratio; need for highest air emissions, more expensive than ATR and POX.	(de Rezende et al. 2015; Xu et al. 2022)
DRM $CH_4 + CO_2 \rightarrow 2H_2 + 2CO$	Almost 100% CO_2 conversion, Consumption of GHG: CH_4 and CO_2, generation of syngas with suitable FT ratio although the high temperature of reaction causes agglomeration, coke formation and plugging of the reactor.	(Olah et al. 2013; Serrano-Lotina and Daza 2014; Cunha et al. 2020; Dan et al. 2021)
CSDRM $3CH_4 + CO_2 + 2H_2O \rightarrow 8H_2 + 4CO$ $CH_4 + {}^{1}/_{3}\,CO_2 + {}^{2}/_{3}\,H_2O \rightarrow {}^{8}/_{3}\,H_2 + {}^{4}/_{3}\,CO$	Significant coke reduction; best syngas ratio for liquid fuels production; unreacted CH_4 needs to be separated; installation cost.	(Gangadharan et al. 2012)
POXM $CH_4 + {}^{1}/_{2}\,O_2 \rightarrow CO + 2H_2$	Relatively, low syngas ratio; high reaction temperature (1100–1500); needs pure oxygen plant; no need for sulphur removal from the feedstock.	(Al-Nakoua and El-Naas 2012; Carapellucci and Giordano 2020)
Coke-forming Side reactions		
CO_2 /CO hydrogenation $CO_2 + 2H_2 \leftrightarrow 2H_2O + C_{(s)}$ $CO + H_2 \leftrightarrow H_2O + C_{(s)}$	Ideal for the generation of syngas, aromatics, value-added chemicals, olefins and methanol intermediates. Depending on hydrogen and oxygen availability in the system, hydrogenation (up to C_5), C-C coupling, acid-catalyzed reactions aromatisation, oligomerisation and isomerisation may take place. In all cases, coke is deposited.	(Borisut and Nuchitprasittichai 2019)
CH_4 cracking $CH_4 \leftrightarrow 2H_2 + C_{(s)}$	The prime endothermic side reaction during CH_4 valuation where the C-H (strong) bond breaks to generate H_2 gas and deposit coke (C) in the presence of catalysts, the reaction may surface in the range 450–750 °C while may extend above 1200 °C in uncatalyzed reactions.	(Alves et al. 2021)
Coke hydration/syngas substitution $C + H_2O \leftrightarrow H_2 + CO$	The reaction progresses with a 1:1 ratio either way. However, the forward reaction is more economical and profitable being more inclined towards FT syngas ratio and less coke formation.	(Basu 2018)
CO disproportionation/ BR $2CO \leftrightarrow CO_2 + C_{(s)}$ $C + {}^{1}/_{2}\,O_2 \leftrightarrow CO$	A reversible char-gasification where CO_2 is reduced by the deposit of coke in the reaction to generate CO and vice-versa. Below 1000 K, the char-gasification rate is insignificant, therefore the CO disproportionation is more favoured at these temperatures.	(Horlyck et al. 2018; Azancot et al. 2021)
Non-coke-forming side reactions		
WGS reaction $CO + H_2O \rightarrow CO_2 + H_2$	A moderately exothermic, kinetically limited below 250 °C equilibrium limited high-temperature reaction, for the manufacture of hydrocarbons, methanol, ammonia and hydrogen. It contains over 20% by volume hydrogen and water vapour > 6% by volume.	(Dybkjær and Christensen 2001; Kurdi et al. 2022)
RWGS reaction $CO_2 + H_2 \leftrightarrow CO + H_2O$	A feasible reaction to produce CO and steam from CO_2 and hydrogen. It could be a profitable technique for the generation of oxygen alongside water electrolysis	(Pastor-Pérez et al. 2017)

Table 6 (continued)

Reforming equations	Description/challenges	Ref
Oxidation reactions		
$C+O_2 \rightarrow CO_2$ $C+{}^{1}/_{2}O_2 \rightarrow CO_2$ $CH_4+2O_2 \leftrightarrow CO_2+2H_2O$ $H_2+O_2 \leftrightarrow H_2O$	Mostly endothermic reactions, requiring heat supply, drying and pyrolysis, which produces the fuel gas CO, and around 111 kJ mol^{-1} of heat. Contact with oxygen produces either the predominant CO_2 gas, steam or a mixture of both.	(Basu 2018)
Methanation reactions		
$2CO+2H_2 \leftrightarrow CH_4+CO_2$ $CO+3H_2 \leftrightarrow CH_4+H_2O$ $CO_2+4H_2 \leftrightarrow CH_4+2H_2O$	More toxic and less stable CO could be hydrogenated to produce a mixture of methane and steam, or CO_2. The storage of CH_4 is one of the major challenges and transportation cost.	(Wang et al. 2018a; Hatta et al. 2021; Hussain et al. 2022)

increased quickly before decreasing to a constant state. The thermal and energy storage efficiencies were computed using heat loss, which is minimal at low temperatures, and phase transition enthalpy, which increases storage efficiency when solar energy is absorbed (Peng et al. 2022). A summary of findings reported on the recent photothermal conversion of methane is presented in Table 4.

Dual methane reforming (bi-reforming)

The production of syngas through combined steam and dry methane reformation (CSDRM), known as bi-reforming, seems to be a highly promising CO_2 valorisation process, providing metgas ($CO + 2H_2$) with an H_2/CO molar ratio close to 2 (Jabbour et al. 2017). This intuitive way (Eq. (9)) achieves a syngas with a desired H_2/CO ratio and combines both DRM (Eq. (1)) and SRM (Eq. (7)) processes (Singh et al. 2017; Jabbour 2020). For example, specific FT procedures are designed to prepare long hydrocarbon chains, while they may be utilised directly in methanol (Hatta et al. 2023) or dimethyl ether (Owgi et al. 2023a; Nabgan et al. 2023) synthesis. Conventional DRM (Eq. (1)) and SRM (Eq. (7)) give an H_2/CO ratio of almost 1 (too low) or nearly 3 (too high), requiring additional cycles (often expensive) if the product ratio needs to be changed to be around 2 for the following stages of the process.

$$3CH_4 + CO_2 + 2H_2O \rightarrow 8H_2 + 4CO \quad \Delta H^0{}_{298\,K} = +220\ kJmol^{-1} \tag{9}$$

From a practical standpoint, the CSDRM process has the added benefit of utilising CH_4, CO_2, and water as its principal reactants. These gases can also be present in biogas, a fuel that does not derive from fossil fuels. As a result, the approach's complex development provides a way for creating metgas from renewable energy sources without using additional separation and purifying processes. Recent progress in the field emphasises more on combined reforming because it consumes more CH_4 than conventional reforming processes in which water has been reported to ignite side reactions. When DRM and SRM are combined with water, as in (Eq. (9)) above, less carbon may accumulate on the catalyst surface and more H_2 will be produced, resulting in syngas with the ideal composition for synthetic fuels (Dan et al. 2021). Table 5 summarises performing conditions, methods and catalyst systems in combined reforming reactions.

The fate of captured gaseous species (based on previous investigations)

Gasifier updraft stages include combustion, gasification, pyrolysis and drying zones. In the drying zone, the product gas is liberated and burns with the fuels; in the pyrolysis zone, dry fuel (char + volatiles) is produced; and the gasification zone involves the conversion of coke and CO based on the reactions:

$$C + CO_2 = 2CO \tag{10}$$

$$C + H_2O = CO + H_2 \tag{11}$$

$$C + 2H_2 = CH_4 \tag{12}$$

$$CO + H_2O = CO_2 + H_2 \tag{13}$$

In the combustion zone, CO and CO_2 are made when partial and complete coke oxidation happens. Table 6 shows the different reactions of gaseous species.

Future prospective

Finding more efficient ways to produce syngas has received a lot of attention recently since it is a necessary intermediary in producing several chemicals and fuels, including dimethyl

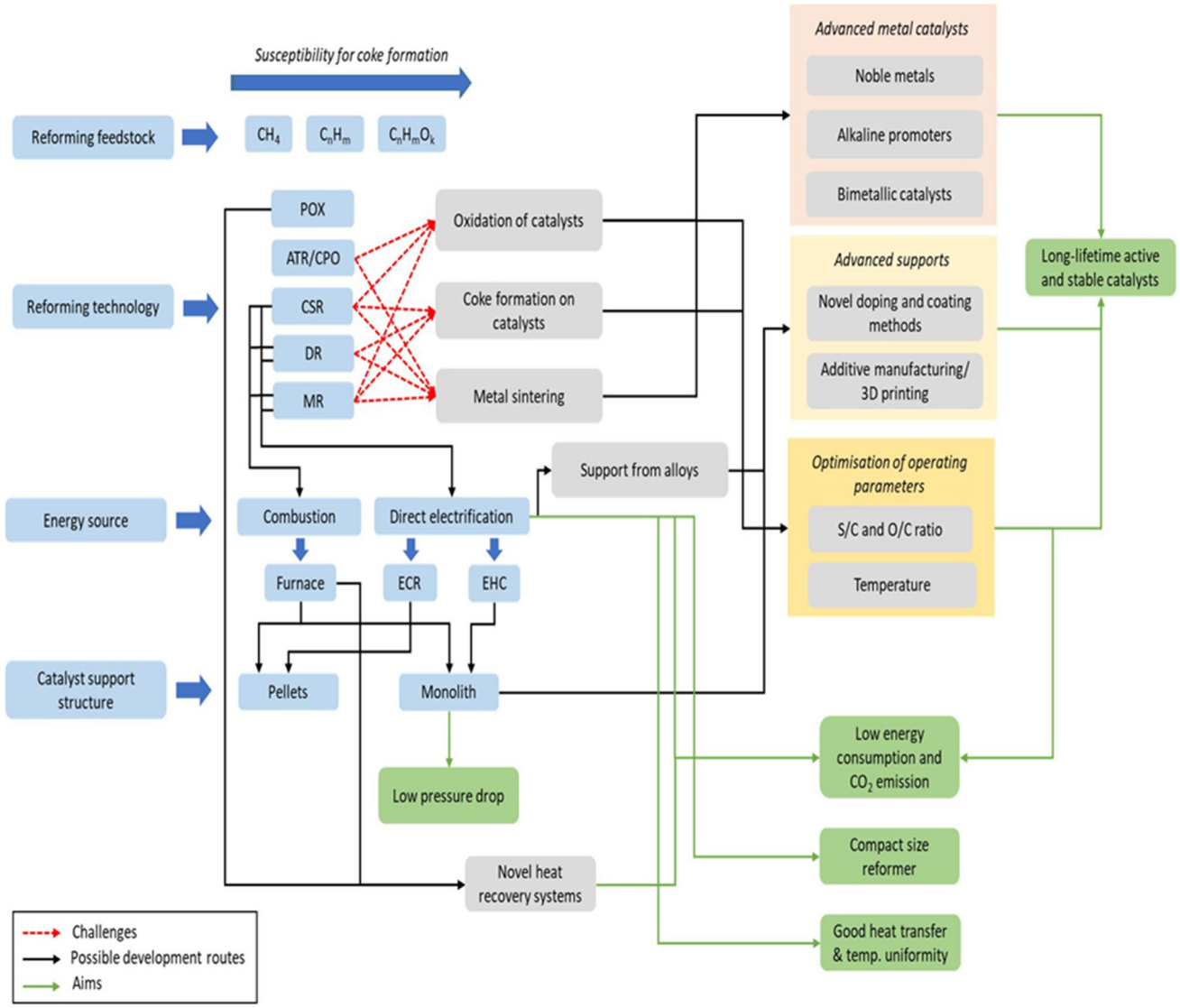

Fig. 9 The challenges and potential paths for reformer development are based on the progress and status of various reformer technologies in related studies (reused with permission from the reference (Bolívar Caballero et al. 2022))

ether, methanol, propylene, ethylene and FT fuels. Using waste CO_2, DRM transforms natural gas into syngas. For some years, the industry has used a mix of steam and dry methane reforming (SMR + DRM) instead of DRM, which has yet to be fully industrialised (Bahari et al. 2022; Owgi et al. 2023b).

Maximizing reaction temperatures is crucial for enhancing product conversions, especially in the context of DRM, a process essential for reducing GHG emissions. However, increased temperatures also result in enhanced conversion rates, highlighting the potential for improved efficiency in hydrogen and synfuel production. It is important to note the challenges associated with lower DRM temperatures, such as the production of high-water content streams and the promotion of endothermic processes like RWGS. While DRM and RWGS methods are important for hydrogen and synfuel production, there is a growing recognition of the significance of other reforming processes, such as SR and carbon gasification. These processes require significant amounts of water but provide alternative methods for synthesising products and enhance the overall adaptability of hydrogen and synfuel generation.

Despite the benefits of higher temperatures and diverse reforming procedures, achieving high selectivity for hydrogen production remains challenging, especially when the CO_2/CH_4 ratio exceeds 1. The predominance of the RWGS reaction in these circumstances leads to reduced specificity for hydrogen, highlighting the need for innovative approaches to enhance product distribution. The emergence of triple-methane reforming reactors represents

significant progress in addressing the challenges associated with conventional reforming procedures. These reactors utilise steam, oxygen and photothermal DRM systems to overcome issues such as excessive coking, agglomeration and uneven distribution of reactants and products. Moreover, current research efforts focus on optimising reactor design to increase efficiency, reduce energy demands and improve overall process control.

The development and improvement of catalysts are also crucial areas of focus for future studies. Durable, efficient and cost-effective catalysts are necessary for the generation of valuable chemicals from CH_4 and CO_2. Through current characterisation and computational modelling techniques, researchers aim to understand catalyst performance better. Further research and innovation are needed to fully harness the potential of hydrogen and synfuel generation. By strategically incorporating emerging trends, employing advanced methodologies and fostering interdisciplinary collaboration, it is possible to effectively tackle existing challenges and establish a resilient and sustainable energy future. Figure 9 presents the challenges and potential paths for the development of reformer technologies, based on the progress and status of various reformer technologies reviewed in related studies.

Conclusion

This article has covered all the many methods for valuing methane, including dry, auto-thermal, steam, photothermal and partial oxidation techniques. Carbon capture and utilisation (CCU) and carbon capture and storage (CCS) are two carbon management mechanisms that have recently received a lot of attention from researchers concerned about the effects of human-caused emissions of greenhouse gases on the environment.

Methane reforming via water electrolysis, a method that currently accounts for a mere 5% of the overall production of hydrogen, has been an area of considerable discourse. Although the process of converting CO_2 into fuels and compounds shows potential for a future without carbon emissions, the complete eradication of carbon-based products continues to present difficulties. As a result, it is critical to embrace a well-rounded strategy that combines the use of carbon-based resources with the conscientious management of atmospheric CO_2 through the establishment of a human carbon cycle. Chemical hydrogen looping, biomass pyrolysis and coke oven gas utilisation are just a few of the novel approaches that have recently emerged and show promise as a means of producing energy sustainably. However, it is critical to address the energy requirements associated with methane abatement, as well as problems related to storage, transportation and manufacturing.

Future studies should focus on making methane valorisation technologies more efficient and scalable. Motivating the adoption of carbon-neutral practices and promoting the integration of renewable energy sources into existing infrastructure should be the focus of collaborative initiatives including academia, industry and policymakers. To further drive innovation in this crucial sector, interdisciplinary techniques that utilise materials science, chemistry and engineering insights are necessary. Through the progression of knowledge regarding methane valorisation and carbon management, it is possible to establish a pathway towards an energy future that is more resilient and sustainable, all while alleviating the detrimental effects of greenhouse gas emissions on both the environment and human health.

Acknowledgements The authors gratefully acknowledge the Universiti Teknologi Malaysia High Impact Research Grant (VOT No.: 08G92). The first author is thankful to the Tertiary Education Trust Fund (TETfund, Nigeria) and the management of Sokoto State University, Sokoto, for the study opportunity.

Author contribution The study's inception and design were contributed to by all authors. MA, AHKO, WN and AHH prepared the materials, collected data and analyzed the results. MA, NFBK, MBB and TVT wrote the first draught of the manuscript. AAA and BBN provided feedback on prior draught. MYSH gave comments and proofread. AAJ secured the funding and supervised. The final manuscript was read and approved by all authors.

Funding This work was supported by the Universiti Teknologi Malaysia High Impact Research Grant (VOT No.: 08G92).

Data availability Not applicable

Declarations

Ethics approval and consent to participate Not applicable

Consent for publish Not applicable

Competing interests The authors declare no competing interests.

References

Abbas T, Tahir M (2021) Tri-metallic Ni–Co modified reducible TiO2 nanocomposite for boosting H2 production through steam reforming of phenol. Int J Hydrog Energy 46:8932–8949. https://doi.org/10.1016/j.ijhydene.2020.12.209

Abdelkareem MA, Soudan B, Mahmoud MS et al (2022) Progress of artificial neural networks applications in hydrogen production. Chem Eng Res Des 182:66–86. https://doi.org/10.1016/j.cherd.2022.03.030

Afzal S, Prakash AV, Littlewood P et al (2020) Controlling the rate of change of Ni dispersion in commercial catalyst by ALD overcoat during dry reforming of methane. Int J Hydrog Energy 45:12835–12848. https://doi.org/10.1016/j.ijhydene.2020.03.008

Ahmad MI, Zhang N, Jobson M (2011) Integrated design of diesel hydrotreating processes. Chem Eng Res Des 89:1025–1036. https://doi.org/10.1016/j.cherd.2010.11.021

Ahmed IA, Hussein HS, Ragab AH, Al-Radadi NS (2020) Synthesis and characterization of silica-coated oxyhydroxide aluminum/doped polymer nanocomposites: a comparative study and its application as a sorbent. Molecules 25:1520. https://doi.org/10.3390/MOLECULES25071520

Ahn K, Chung YC, Oh JH et al (2011) A comparative study of catalytic partial oxidation of methane over CeO 2 supported metallic catalysts. J Nanosci Nanotechnol 11:6414–6419. https://doi.org/10.1166/jnn.2011.4383

Alabi WO, Sulaiman KO, Wang H et al (2020) Effect of spinel inversion and metal-support interaction on the site activity of Mg-Al-Ox supported Co catalyst for CO2 reforming of CH4. J CO2 Util 37:180–187. https://doi.org/10.1016/j.jcou.2019.12.006

Alhassan M, Faruq UZ, Galadima A (2019) Mixed-metal oxide catalyst for liquid phase benzene alkylation. Earthline J Chem Sci 2(2):217–234. https://doi.org/10.34198/ejcs.2219.217234

Alhassan M, Jalil AA, Nabgan W et al (2022) Bibliometric studies and impediments to valorization of dry reforming of methane for hydrogen production. Fuel 328. https://doi.org/10.1016/j.fuel.2022.125240

Alhassan M, Jalil AA, Bahari MB et al (2023) RSC Advances REVIEW support interactions. RSC Adv 13:1711–1726. https://doi.org/10.1039/D2RA06773K

Alhassan M, Jalil AA, Omoregie AI et al (2024) Silica-based materials in methane conversion: a two-decade bibliometric and literature review (1995–2022). Top Catal. https://doi.org/10.1007/s11244-024-01932-w

Ali S, Gamal A, Khader MM (2023) Development of highly active and coke-resilient Ni-based catalysts for low-temperature steam reformation of methane. Catal Commun 175:106605. https://doi.org/10.1016/j.catcom.2023.106605

Al-Nakoua MA, El-Naas MH (2012) Combined steam and dry reforming of methane in narrow channel reactors. Int J Hydrog Energy 37:7538–7544. https://doi.org/10.1016/j.ijhydene.2012.02.031

Alves L, Pereira V, Lagarteira T, Mendes A (2021) Catalytic methane decomposition to boost the energy transition: scientific and technological advancements. Renew Sust Energ Rev 137. https://doi.org/10.1016/j.rser.2020.110465

Araiza DG, Arcos DG, Gómez-Cortés A, Díaz G (2021) Dry reforming of methane over Pt-Ni/CeO2 catalysts: effect of the metal composition on the stability. Catal Today 360:46–54. https://doi.org/10.1016/j.cattod.2019.06.018

Arku P, Regmi B, Dutta A (2018) A review of catalytic partial oxidation of fossil fuels and biofuels: recent advances in catalyst development and kinetic modelling. Chem Eng Res Des 136:385–402. https://doi.org/10.1016/j.cherd.2018.05.044

Avci AK, Önsan ZI (2018) Catalysts.https://doi.org/10.1016/B978-0-12-809597-3.00235-2

Aw MS, Osojnik Črnivec IG, Djinović P, Pintar A (2014) Strategies to enhance dry reforming of methane: synthesis of ceria-zirconia/nickel-cobalt catalysts by freeze-drying and NO calcination. Int J Hydrog Energy 39:12636–12647. https://doi.org/10.1016/j.ijhydene.2014.06.083

Azancot L, Bobadilla LF, Centeno MA, Odriozola JA (2021) IR spectroscopic insights into the coking-resistance effect of potassium on nickel-based catalyst during dry reforming of methane. Appl Catal B:285. https://doi.org/10.1016/j.apcatb.2020.119822

Baamran KS, Tahir M (2019) Ni-embedded TiO2-ZnTiO3 reducible perovskite composite with synergistic effect of metal/support towards enhanced H2 production via phenol steam reforming. Energy Convers Manag 200:112064. https://doi.org/10.1016/j.enconman.2019.112064

Bahaghighat HD, Freye CE, Synovec RE (2019) Recent advances in modulator technology for comprehensive two dimensional gas chromatography. TrAC - Trends Analyt Chem 113:379–391. https://doi.org/10.1016/j.trac.2018.04.016

Bahari MB, Mamat CR, Jalil AA et al (2022) Enriching the methanol generation via CO2 photoconversion over the cockscomb-like fibrous silica copper. Fuel 328. https://doi.org/10.1016/j.fuel.2022.125257

Bahari MB, Setiabudi HD, Nguyen TD et al (2021) Hydrogen production via CO2[sbnd]CH4 reforming over cobalt-supported mesoporous alumina: a kinetic evaluation. Int J Hydrog Energy 46:24742–24753. https://doi.org/10.1016/j.ijhydene.2020.04.130

Basu P (2018) Gasification theory. https://doi.org/10.1016/B978-0-12-812992-0.00007-8

Batuecas E, Liendo F, Tommasi T et al (2021) Recycling CO2from flue gas for CaCO3nanoparticles production as cement filler: a Life Cycle Assessment. J CO2 Util 45. https://doi.org/10.1016/j.jcou.2021.101446

Bian Z, Suryawinata IY, Kawi S (2016) Highly carbon resistant multicore-shell catalyst derived from Ni-Mg phyllosilicate nanotubes@silica for dry reforming of methane. Appl Catal B 195:1–8. https://doi.org/10.1016/j.apcatb.2016.05.001

Bolívar Caballero JJ, Zaini IN, Yang W (2022) Reforming processes for syngas production: a mini-review on the current status, challenges, and prospects for biomass conversion to fuels. Appl Energy Combust Sci 10. https://doi.org/10.1016/j.jaecs.2022.100064

Boretti A, Dorrington G (2013) Are synthetic liquid hydrocarbon fuels the future of more sustainable aviation in Australia? Int J Hydrog Energy 38:14832–14836. https://doi.org/10.1016/j.ijhydene.2013.09.042

Borisut P, Nuchitprasittichai A (2019) Methanol production via CO2 hydrogenation: sensitivity analysis and simulation—based optimization. Front Energy Res 7:1–10. https://doi.org/10.3389/fenrg.2019.00081

British Petroleum (2021) Statistical Review of World Energy 2021. BP Energy Outlook 2021 70:8–20

Bruhn T, Naims H, Olfe-Kräutlein B (2016) Separating the debate on CO2 utilisation from carbon capture and storage. Environ Sci Pol 60:38–43. https://doi.org/10.1016/j.envsci.2016.03.001

Cao D, Luo C, Luo T et al (2024) Dry reforming of methane by La2NiO4 perovskite oxide: B-site substitution improving reactivity and stability. Chem Eng J 482:148701. https://doi.org/10.1016/j.cej.2024.148701

Carapellucci R, Giordano L (2020) Steam, dry and autothermal methane reforming for hydrogen production: a thermodynamic equilibrium analysis. J Power Sources 469:228391. https://doi.org/10.1016/j.jpowsour.2020.228391

Chai SYW, Ngu LH, How BS (2022) Review of carbon capture absorbents for CO2 utilization. Greenh Gases: Sci Technol 12:394–427. https://doi.org/10.1002/ghg.2151

Charisiou ND, Siakavelas G, Papageridis KN et al (2016) Syngas production via the biogas dry reforming reaction over nickel supported on modified with CeO2 and/or La2O3 alumina catalysts. J Nat Gas Sci Eng 31:164–183. https://doi.org/10.1016/j.jngse.2016.02.021

Chaudhary PK, Koshta N, Deo G (2020) Effect of O2 and temperature on the catalytic performance of Ni/Al2O3 and Ni/MgAl2O4 for the dry reforming of methane (DRM). Int J Hydrog Energy 45:4490–4500. https://doi.org/10.1016/j.ijhydene.2019.12.053

Cheephat C, Daorattanachai P, Devahastin S, Laosiripojana N (2018) Partial oxidation of methane over monometallic and bimetallic Ni-, Rh-, Re-based catalysts: Effects of Re addition, co-fed reactants and catalyst support. Appl Catal A Gen 563:1–8. https://doi.org/10.1016/j.apcata.2018.06.032

Chen G, Dong X, Yan B et al (2022) Photothermal steam reforming : a novel method for tar elimination in biomass gasification. Appl Energy 305:117917. https://doi.org/10.1016/j.apenergy.2021.117917

Chen J, Sun J, Wang Y (2017) Catalysts for steam reforming of bio-oil: a review. Ind Eng Chem Res 56:4627–4637. https://doi.org/10.1021/ACS.IECR.7B00600

Chen L, Qi Z, Zhang S, Su J, Somorjai GA (2020) Catalytic hydrogen production from methane: a review on recent progress and prospect. Catalysts 10:858. https://doi.org/10.3390/catal10080858

Chen Q, Lv M, Tang Z et al (2016) Opportunities of integrated systems with CO2 utilization technologies for green fuel & chemicals production in a carbon-constrained society. J CO2 Util 14:1–9. https://doi.org/10.1016/j.jcou.2016.01.004

Chong CC, Bukhari SN, Cheng YW et al (2019) Robust Ni/dendritic fibrous SBA-15 (Ni/DFSBA-15) for methane dry reforming: effect of Ni loadings. Appl Catal A Gen 584. https://doi.org/10.1016/j.apcata.2019.117174

Cuéllar-Franca RM, Azapagic A (2015) Carbon capture, storage and utilisation technologies: a critical analysis and comparison of their life cycle environmental impacts. J CO2 Util 9:82–102. https://doi.org/10.1016/j.jcou.2014.12.001

Cunha AF, Mata TM, Caetano NS et al (2020) Catalytic bi-reforming of methane for carbon dioxide ennoblement. Energy Rep 6:74–79. https://doi.org/10.1016/j.egyr.2019.08.022

Dan M, Mihet M, Borodi G, Lazar MD (2021) Combined steam and dry reforming of methane for syngas production from biogas using bimodal pore catalysts. Catal Today 366:87–96. https://doi.org/10.1016/j.cattod.2020.09.014

Das S, Sengupta M, Patel J, Bordoloi A (2017) A study of the synergy between support surface properties and catalyst deactivation for CO2 reforming over supported Ni nanoparticles. Appl Catal A Gen 545:113–126. https://doi.org/10.1016/J.APCATA.2017.07.044

de Rezende SM, Franchini CA, Dieuzeide ML et al (2015) Glycerol steam reforming over layered double hydroxide-supported Pt catalysts. Chem Eng J 272:108–118. https://doi.org/10.1016/j.cej.2015.03.033

Dinani AM, Nassaji A, Hamzehlouyan T (2023) An optimized economic-environmental model for a proposed flare gas recovery system. Energy Rep 9:2921–2934. https://doi.org/10.1016/j.egyr.2023.01.103

Doğan Özcan M, Akın AN (2023) Influence of silica promotion on NiCe/MgAlSi catalysts for the oxy-steam reforming of biogas to syngas. Int J Hydrog Energy. https://doi.org/10.1016/j.ijhydene.2023.02.089

Dutta PK, Vaidyalingam AS (2003) Zeolite-supported ruthenium oxide catalysts for photochemical reduction of water to hydrogen. Microporous Mesoporous Mater 62:107–120. https://doi.org/10.1016/S1387-1811(03)00399-8

Dybkjær I, Christensen TS (2001) Syngas for large scale conversion of natural gas to liquid fuels. Stud Surf Sci Catal 136:435–440. https://doi.org/10.1016/s0167-2991(01)80342-6

El Hakim S, Chave T, Nada AA et al (2021) Tailoring noble metal-free Ti @ TiO 2 photocatalyst for boosting photothermal hydrogen production. Front Catal 1:1–10. https://doi.org/10.3389/fctls.2021.669260

Elbadawi AH, Ge L, Li Z et al (2021) Catalytic partial oxidation of methane to syngas: review of perovskite catalysts and membrane reactors. Catal Rev Sci Eng 63:1–67. https://doi.org/10.1080/01614940.2020.1743420

Elvidge CD, Zhizhin M, Baugh K et al (2015) Methods for global survey of natural gas flaring from visible infrared imaging radiometer suite data. Energies 9(1):14. https://doi.org/10.3390/en9010014

Farniaei M, Abbasi M, Rahnama H et al (2014) Syngas production in a novel methane dry reformer by utilizing of tri-reforming process for energy supplying: Modeling and simulation. J Nat Gas Sci Eng 20:132–146. https://doi.org/10.1016/j.jngse.2014.06.010

Fazlikeshteli S, Vendrell X, Llorca J (2021) Low-temperature methane partial oxidation over Pd supported on CeO2: effect of the preparation method and precursors. Reactions 2:30–42. https://doi.org/10.3390/reactions2010004

Fisher D, Wooster MJ (2019) Remote sensing of environment multi-decade global gas flaring change inventoried using the ATSR-1 , ATSR-2 , AATSR and SLSTR data records. Remote Sens Environ 232:111298. https://doi.org/10.1016/j.rse.2019.111298

Gangadharan P, Kanchi KC, Lou HH (2012) Evaluation of the economic and environmental impact of combining dry reforming with steam reforming of methane. Chem Eng Res Des 90:1956–1968. https://doi.org/10.1016/j.cherd.2012.04.008

Gao Y, Jiang J, Meng Y et al (2018) A review of recent developments in hydrogen production via biogas dry reforming. Energy Convers Manag 171:133–155. https://doi.org/10.1016/j.enconman.2018.05.083

Gao X, Lin Z, Li T, Huang L, Zhang J, Askari S, Dewangan N, Jangam A, Kawi S (2021)Recent developments in dielectric barrier discharge plasma-assisted catalytic dry reforming of methane over ni-based catalysts. Catalysts 11:455. https://doi.org/10.3390/catal11040455

Goula MA, Charisiou ND, Siakavelas G et al (2017) Syngas production via the biogas dry reforming reaction over Ni supported on zirconia modified with CeO2 or La2O3 catalysts. Int J Hydrog Energy 42:13724–13740. https://doi.org/10.1016/j.ijhydene.2016.11.196

Guo X, Sun Y, Yu Y et al (2012) Carbon formation and steam reforming of methane on silica supported nickel catalysts. Catal Commun 19:61–65. https://doi.org/10.1016/j.catcom.2011.12.031

Habimana F, Li X, Ji S et al (2009) Effect of Cu promoter on Ni-based SBA-15 catalysts for partial oxidation of methane to syngas. J Nat Gas Chem 18:392–398. https://doi.org/10.1016/S1003-9953(08)60130-9

Han K, Wang Y, Wang S et al (2021) Narrowing band gap energy of CeO2 in (Ni/CeO2)@ SiO2 catalyst for photothermal methane dry reforming. Chem Eng J 421:129989

Hatta AH, Jalil AA, Hassan NS et al (2021) ScienceDirect A review on recent bimetallic catalyst development for synthetic natural gas production via CO methanation. Int J Hydrog Energy 47:30981–31002. https://doi.org/10.1016/j.ijhydene.2021.10.213

Hatta AH, Jalil AA, Hassan NS et al (2023) A short review on informetric analysis and recent progress on contribution of ceria in Ni-based catalysts for enhanced catalytic CO methanation. Powder Technol 417:118246. https://doi.org/10.1016/j.powtec.2023.118246

He C, Wu S, Wang L, Zhang J (2022) Recent advances in photo-enhanced dry reforming of methane: a review. J Photochem Photobiol C: Photochem Rev 51:100468. https://doi.org/10.1016/j.jphotochemrev.2021.100468

He X, Liu L (2017) Thermodynamic analysis on the CO2 conversion processes of methane dry reforming for hydrogen production and CO2 hydrogenation to dimethyl ether. IOP Conf Ser Earth Environ Sci 100:1–9. https://doi.org/10.1088/1755-1315/100/1/012078

Horlyck J, Lawrey C, Lovell EC et al (2018) Elucidating the impact of Ni and Co loading on the selectivity of bimetallic NiCo catalysts for dry reforming of methane. Chem Eng J 352:572–580. https://doi.org/10.1016/j.cej.2018.07.009

Hou Z, Gao J, Guo J et al (2007) Deactivation of Ni catalysts during methane autothermal reforming with CO2 and O2 in a fluidized-bed reactor. J Catal 250:331–341. https://doi.org/10.1016/j.jcat.2007.06.023

Howarth RW, Jacobson MZ (2021) How green is blue hydrogen ? Energy Sci Eng 9(10):1676–1687. https://doi.org/10.1002/ese3.956

Hussain I, Jalil AA, Hassan NS et al (2022) Contemporary thrust and emerging prospects of catalytic systems for substitute natural

gas production by CO methanation. Fuel 311. https://doi.org/10.1016/J.FUEL.2021.122604
Ibrahim AA, Al-Fatesh AS, Khan WU et al (2019) Enhanced coke suppression by using phosphate-zirconia supported nickel catalysts under dry methane reforming conditions. Int J Hydrog Energy 44:27784–27794. https://doi.org/10.1016/j.ijhydene.2019.09.014
Ibrahim AA, Fakeeha AH, Lanre MS et al (2022) The effect of calcination temperature on various sources of ZrO 2 supported Ni catalyst for dry reforming of methane. Catalysts 12(4):361
Ighalo JO, Amama PB (2024) Recent advances in the catalysis of steam reforming of methane (SRM). Int J Hydrog Energy 51:688–700
Ismagilov IZ, Matus EV, Kuznetsov VV et al (2014) Hydrogen production by autothermal reforming of methane over NiPd catalysts: effect of support composition and preparation mode. Int J Hydrog Energy 39:20992–21006. https://doi.org/10.1016/j.ijhydene.2014.10.044
Jabbour K (2020) Tuning combined steam and dry reforming of methane for "metgas" production: a thermodynamic approach and state-of-the-art catalysts. J Energy Chem 48:54–91
Jabbour K, Massiani P, Davidson A et al (2017) Ordered mesoporous "one-pot" synthesized Ni-Mg(Ca)-Al2O3 as effective and remarkably stable catalysts for combined steam and dry reforming of methane (CSDRM). Appl Catal B 201:527–542. https://doi.org/10.1016/j.apcatb.2016.08.009
Javed AH, Shahzad N, Butt FA et al (2021) Synthesis of bimetallic Co-Ni/ZnO nanoprisms (ZnO-NPr) for hydrogen-rich syngas production via partial oxidation of methane. J Environ Chem Eng 9. https://doi.org/10.1016/j.jece.2021.106887
Jin B, Li S, Liang X (2021) Enhanced activity and stability of MgO-promoted Ni/Al2O3 catalyst for dry reforming of methane: Role of MgO. Fuel 284. https://doi.org/10.1016/j.fuel.2020.119082
Johannsen RM, Mathiesen BV, Kermeli K et al (2023) Exploring pathways to 100% renewable energy in European industry. Energy 268. https://doi.org/10.1016/j.energy.2023.126687
Karakaya M, Ilsen Onsan Z, Avci AK (2013) Microchannel autothermal reforming of methane to synthesis gas. Top Catal 56:1716–1723. https://doi.org/10.1007/s11244-013-0107-1
Khajenoori M, Rezaei M, Nematollahi B (2013) Preparation of noble metal nanocatalysts and their applications in catalytic partial oxidation of methane. J Ind Eng Chem 19:981–986. https://doi.org/10.1016/j.jiec.2012.11.020
Kim P, Kim Y, Kim H et al (2004) Synthesis and characterization of mesoporous alumina with nickel incorporated for use in the partial oxidation of methane into synthesis gas. Appl Catal A Gen 272:157–166. https://doi.org/10.1016/j.apcata.2004.05.055
Kim TY, Kim SM, Lee WS, Woo SI (2013) Effect and behavior of cerium oxide in Ni/γ-Al2O 3 catalysts on autothermal reforming of methane: CeAlO3 formation and its role on activity. Int J Hydrog Energy 38:6027–6032. https://doi.org/10.1016/j.ijhydene.2012.12.115
Kim WY, Jang JS, Ra EC et al (2019) Reduced perovskite LaNiO3 catalysts modified with Co and Mn for low coke formation in dry reforming of methane. Appl Catal A Gen 575:198–203. https://doi.org/10.1016/j.apcata.2019.02.029
Kong LT, Zhang M, Liu X et al (2019) Green and rapid synthesis of iron molybdate catalyst by mechanochemistry and their catalytic performance for the oxidation of methanol to formaldehyde. Chem Eng J 364:390–400. https://doi.org/10.1016/j.cej.2019.01.164
Kurdi AN, Ibrahim AA, Al-Fatesh AS et al (2022) Hydrogen production from CO 2 reforming of methane using zirconia supported nickel catalyst. RSC Adv 12(17):10846–10854. https://doi.org/10.1039/d2ra00789d
Laosiripojana N, Assabumrungrat S (2007) Catalytic steam reforming of methane, methanol, and ethanol over Ni/YSZ: The possible use of these fuels in internal reforming SOFC. J Power Sources 163:943–951. https://doi.org/10.1016/j.jpowsour.2006.10.006
Lara Sandoval AE, Serafin J, Murcia Mesa JJ et al (2024) Evaluation of Pt/TiO2-Nb2O5 systems in the photocatalytic reforming of glucose for the generation of H2 from industrial effluents. Fuel 363:130932. https://doi.org/10.1016/j.fuel.2024.130932
Lee CH, Kwon BW, Oh JH et al (2022) Integration of dry-reforming and sorption-enhanced water gas shift reactions for the efficient production of high-purity hydrogen from anthropogenic greenhouse gases. J Ind Eng Chem 105:563–570. https://doi.org/10.1016/j.jiec.2021.10.016
Li B, Maruyama K, Nurunnabi M et al (2004) Temperature profiles of alumina-supported noble metal catalysts in autothermal reforming of methane. Appl Catal A Gen 275:157–172. https://doi.org/10.1016/j.apcata.2004.07.047
Li B, Xu X, Zhang S (2013) Synthesis gas production in the combined CO2 reforming with partial oxidation of methane over Ce-promoted Ni/SiO2 catalysts. Int J Hydrog Energy 38:890–900. https://doi.org/10.1016/j.ijhydene.2012.10.103
Li B, Yuan X, Li L et al (2021) Lanthanide oxide modified nickel supported on mesoporous silica catalysts for dry reforming of methane. Int J Hydrog Energy 46:31608–31622. https://doi.org/10.1016/j.ijhydene.2021.07.056
Li L, Chen J, Wang S et al (2019) Utilization of biochar for a process of methane dry reforming coupled with steam gasification under microwave heating. J Clean Prod 237:117838. https://doi.org/10.1016/j.jclepro.2019.117838
Li L, Chen J, Zhang Y et al (2022) Ni-Co bimetallic catalysts on coconut shell activated carbon prepared using solid-phase method for highly efficient dry reforming of methane. Environ Sci Pollut Res. https://doi.org/10.1007/s11356-021-18178-8
Li L, Yang Z, Chen J et al (2018) Performance of bio-char and energy analysis on CH4 combined reforming by CO2 and H2O into syngas production with assistance of microwave. Fuel 215:655–664. https://doi.org/10.1016/j.fuel.2017.11.107
Liander,H (1929) Gases Utilisation. Ammonia Process 462:462–472
Lisboa JS, Terra LE, Silva PRJ et al (2011) Investigation of Ni/Ce-ZrO2 catalysts in the autothermal reforming of methane. Fuel Process Technol 92:2075–2082. https://doi.org/10.1016/j.fuproc.2011.06.011
Liu ZW, Jun KW, Roh HS et al (2002) Partial oxidation of methane over nickel catalysts supported on various aluminas. Korean J Chem Eng 19:735–741. https://doi.org/10.1007/BF02706961
Lu L, Lv M, Liu G, Xu X (2017) Photocatalytic hydrogen production over solid solutions between BiFeO 3 and SrTiO 3. Appl Surf Sci 391:535–541. https://doi.org/10.1016/j.apsusc.2016.06.160
Lu Y, Xue J, Yu C et al (1998) Mechanistic investigations on the partial oxidation of methane to synthesis gas over a nickel-on-alumina catalyst. Appl Catal A Gen 174:121–128. https://doi.org/10.1016/S0926-860X(98)00163-X
Lucrédio AF, Jerkiewicz G, Assaf EM (2007) Nickel catalysts promoted with cerium and lanthanum to reduce carbon formation in partial oxidation of methane reactions. Appl Catal A Gen 333:90–95. https://doi.org/10.1016/j.apcata.2007.09.009
Ma Y, Ma Y, Long G et al (2019) Synergistic promotion effect of MgO and CeO2 on nanofibrous Ni/Al2O3 catalysts for methane partial oxidation. Fuel 258:116103. https://doi.org/10.1016/j.fuel.2019.116103
Makertiharta IGBN, Rizki Z, Zunita M, Dharmawijaya PT (2017) Simulation of water gas shift zeolite membrane reactor. IOP Conf Ser Mater Sci Eng 214. https://doi.org/10.1088/1757-899X/214/1/012013
Matas Güell B, Babich IV, Lefferts L, Seshan K (2011) Steam reforming of phenol over Ni-based catalysts - a comparative study. Appl Catal B 106:280–286. https://doi.org/10.1016/j.apcatb.2011.05.012

Meloni E, Martino M, Palma V (2020) A short review on Ni based catalysts and related engineering issues for methane steam reforming. Catalysts 10. https://doi.org/10.3390/catal10030352

Menon MP, Selvakumar R (2017) Derived from biomass for environmental:42750–42773. https://doi.org/10.1039/C7RA06713E

Ming Q, Healey T, Allen L, Irving P (2002) Steam reforming of hydrocarbon fuels. Catal Today 77:51–64. https://doi.org/10.1016/S0920-5861(02)00232-8

Muraza O, Galadima A (2015) A review on coke management during dry reforming of methane. Int J of Energy Res 39(9):1196–1216. https://doi.org/10.1002/er.3295

Nabgan W, Nabgan B, Amran T, Abdullah T (2019) ScienceDirect Conversion of polyethylene terephthalate plastic waste and phenol steam reforming to hydrogen and valuable liquid fuel : Synthesis effect of Ni e Co / ZrO 2 nanostructured catalysts. Int J Hydrog Energy 45:6302–6317. https://doi.org/10.1016/j.ijhydene.2019.12.103

Nabgan W, Nabgan B, Ikram M et al (2022) Synthesis and catalytic properties of calcium oxide obtained from organic ash over a titanium nanocatalyst for biodiesel production from dairy scum. Chemosphere 290:133296. https://doi.org/10.1016/j.chemosphere.2021.133296

Nabgan W, Ikram M, Alhassan M, Owgi AHK, Van Tran T, Parashuram L, Nordin AH, Djellabi R, Jalil AA, Medina F, Nordin ML (2023) Bibliometric analysis and an overview of the application of the non-precious materials for pyrolysis reaction of plastic waste. Arab J Chem 16(6):104717. https://doi.org/10.1016/j.arabjc.2023.104717

Nath N, Chakroborty S, Panda P, Pal K (2022) High Yield Silica-Based Emerging Nanoparticles Activities for Hybrid Catalyst Applications. Top Catal 65:1706–1718. https://doi.org/10.1007/s11244-022-01623-4

Ni C, Pan L, Yuan Z et al (2014) Study of methane autothermal reforming catalyst. J Rare Earths 32:184–188. https://doi.org/10.1016/S1002-0721(14)60049-1

Olah GA, Goeppert A, Czaun M, Prakash GKS (2013) Bi-reforming of methane from any source with steam and carbon dioxide exclusively to metgas (CO-2H2) for methanol and hydrocarbon synthesis. J Am Chem Soc 135:648–650. https://doi.org/10.1021/ja311796n

Orisaremi KK, Chan FTS, Fu X, Chung NSH (2023) Maximizing flare gas power generation for the design of an optimal energy mix. J Clean Prod 391. https://doi.org/10.1016/j.jclepro.2023.136164

Orosa A, Zardoya AR (2022) Research on an internal combustion engine with an injected pre- chamber to operate with low methane number fuels for future gas flaring reduction. Energy 253:124096. https://doi.org/10.1016/j.energy.2022.124096

Osman AI, Mehta N, Elgarahy AM et al (2022) Hydrogen production, storage, utilisation and environmental impacts: a review. Springer International Publishing

Owgi AHK, Jalil AA, Aziz MAA et al (2023a) Effect of promoters (Ce, Sr, Cs, and Sm) on the activity and coke formation of FSA support Ni in the dry reforming of methane. Fuel 340. https://doi.org/10.1016/j.fuel.2023.127592

Owgi AHK, Jalil AA, Aziz MAA et al (2023b) The preferable Ni quantity to boost the performance of FSA for dry reforming of methane. Fuel 332:126124. https://doi.org/10.1016/J.FUEL.2022.126124

Papageridis KN, Siakavelas G, Charisiou ND et al (2016) Comparative study of Ni, Co, Cu supported on γ-alumina catalysts for hydrogen production via the glycerol steam reforming reaction. Fuel Process Technol 152:156–175. https://doi.org/10.1016/j.fuproc.2016.06.024

Pastor-Pérez L, Baibars F, Le Sache E et al (2017) CO2 valorisation via reverse water-gas shift reaction using advanced Cs doped Fe-Cu/Al2O3 catalysts. J CO2 Util 21:423–428. https://doi.org/10.1016/j.jcou.2017.08.009

Peña MA, Gómez JP, Fierro JLG (1996) New catalytic routes for syngas and hydrogen production. Appl Catal A Gen 144:7–57. https://doi.org/10.1016/0926-860X(96)00108-1

Peng S, Zhong W, Zhao H et al (2022) ScienceDirect Solar-driven multifunctional Au / TiO 2 @ PCM towards bio-glycerol photothermal reforming hydrogen production and thermal storage. Int J Hydrog Energy. https://doi.org/10.1016/j.ijhydene.2022.03.273

Pirshahid MRB, Alavi SM, Rezaei M et al (2023) Novel highly efficient Ni-based mesoporous alumina-silica supported catalysts for methane dry reforming: Influence of nickel loading. J Energy Inst:110. https://doi.org/10.1016/j.joei.2023.101361

Polychronopoulou K, Fierro JLG, Efstathiou AM (2004) The phenol steam reforming reaction over MgO-based supported Rh catalysts. J Catal 228:417–432. https://doi.org/10.1016/j.jcat.2004.09.016

Puangpetch T, Sreethawong T, Yoshikawa S, Chavadej S (2009) Hydrogen production from photocatalytic water splitting over mesoporous-assembled SrTiO3 nanocrystal-based photocatalysts. J Mol Catal A Chem 312:97–106. https://doi.org/10.1016/j.molcata.2009.07.012

Qingli X, Zhengdong Z, Kai H et al (2021) Ni supported on MgO modified attapulgite as catalysts for hydrogen production from glycerol steam reforming. Int J Hydrog Energy 46:27380–27393. https://doi.org/10.1016/j.ijhydene.2021.06.028

Qiu Y, Chen J, Zhang J (2007) Effect of CeO2 and CaO promoters on ignition performance for partial oxidation of methane over Ni/MgO-Al2O3 catalyst. J Nat Gas Chem 16:148–154. https://doi.org/10.1016/S1003-9953(07)60040-1

Radlik M, Adamowska-Teyssier M, Krztoń A et al (2015) Dry reforming of methane over Ni/Ce0.62Zr0.38O2 catalysts: effect of Ni loading on the catalytic activity and on H2/CO production. C R Chim 18:1242–1249. https://doi.org/10.1016/j.crci.2015.03.008

Rafiee A, Khalilpour KR, Prest J, Skryabin I (2021) Biogas as an energy vector. Biomass and Bioenergy 144:105935. https://doi.org/10.1016/j.biombioe.2020.105935

Rajabloo T, Valee J, Marenne Y et al (2023) Carbon capture and utilization for industrial applications. Energy Rep 9:111–116. https://doi.org/10.1016/j.egyr.2022.12.009

Sagar TV, Lingaiah N, Sai Prasad PS et al (2024) Phase transformation of Zr-modified LaNiO3 perovskite materials: effect of CO2 reforming of methane to syngas. Catalysts 14:91. https://doi.org/10.3390/catal14010091

Saidi M (2018) ScienceDirect Application of catalytic membrane reactor for pure hydrogen production by flare gas recovery as a novel approach. Int J Hydrog Energy 43:14834–14847. https://doi.org/10.1016/j.ijhydene.2018.05.156

Salahi F, Zarei-Jelyani F, Farsi M, Rahimpour MR (2023a) Optimization of hydrogen production by steam methane reforming over Y-promoted Ni/Al2O3 catalyst using response surface methodology. J Energy Inst 108:101208. https://doi.org/10.1016/j.joei.2023.101208

Salahi F, Zarei-Jelyani F, Meshksar M et al (2023b) Application of hollow promoted Ni-based catalysts in steam methane reforming. Fuel 334:126601. https://doi.org/10.1016/j.fuel.2022.126601

Sasidhar KB, Kumar PS, Xiao L (2022) A critical review on the two-stage biohythane production and its viability as a renewable fuel. Fuel 317:123449. https://doi.org/10.1016/j.fuel.2022.123449

Sayed MA, Abukhadra MR, Salam MA et al (2019) Photocatalytic hydrogen generation from raw water using zeolite/polyaniline@Ni2O3 nanocomposite as a novel photo-electrode. Energy 187:115943. https://doi.org/10.1016/j.energy.2019.115943

Sbaaei ES, Ahmed TS (2018) Predictive modeling and optimization for an industrial Coker Complex Hydrotreating unit – development

and a case study. Fuel 212:61–76. https://doi.org/10.1016/j.fuel.2017.10.032
Schulz LA, Kahle LCS, Delgado KH et al (2015) On the coke deposition in dry reforming of methane at elevated pressures. Appl Catal A Gen 504:599–607. https://doi.org/10.1016/j.apcata.2015.03.002
Seelam PK (2013) Hydrogen production by steam reforming of bio-alcohols: the use of conventional and membraneassisted catalytic reactors. https://urn.fi/URN:ISBN:9789526202778
Serrano-Lotina A, Daza L (2014) Influence of the operating parameters over dry reforming of methane to syngas. Int J Hydrog Energy 39:4089–4094. https://doi.org/10.1016/j.ijhydene.2013.05.135
Shi H, Xia M, Lu H et al (2021) Theoretical investigation of the reactivity of flat Ni (111) and stepped Ni (211) surfaces for acetic acid hydrogenation to ethanol. Int J Hydrog Energy 46:15454–15470. https://doi.org/10.1016/j.ijhydene.2021.02.045
Shokoohi Shooli Z, Izadbakhsh A, Sanati AM (2018) Effect of copper and cerium on the performance of Ni-SBA-16 in the partial oxidation of methane. React Kinet Mech Catal 124:873–889. https://doi.org/10.1007/s11144-018-1375-3
Singh S, Nga NTA, Pham TLM et al (2017) Metgas production from Bi-reforming of methane over lamodified santa barbara amorphous-15 supported nickel catalyst. Chem Eng Trans 56:1573–1578. https://doi.org/10.3303/CET1756263
Sittipunsakda O, Kemacheevakul P, Laosiripojana N, Chuangchote S (2021) Photocatalytic Hydrogen Production from Urine Using Sr-Doped TiO2 Photocatalyst with Subsequent Phosphorus Recovery via Struvite Crystallization. Catalysts 11:1012. https://doi.org/10.3390/catal11081012
Song X, Dong X, Yin S et al (2016) Effects of Fe partial substitution of La2NiO4/LaNiO3 catalyst precursors prepared by wet impregnation method for the dry reforming of methane. Appl Catal A Gen 526:132–138. https://doi.org/10.1016/j.apcata.2016.07.024
Sujianto AE (2020) Maintain sustainable development environment : exports of crude petroleum , coal , natural gas and gross domestic product in Indonesia Earth Env Sci 469(1):012098. https://doi.org/10.1088/1755-1315/469/1/012098
Swaan HM, Rouanet R, Widyananda P et al (1997) Partial oxidation of methane over nickel- and cobalt-based catalysts. In: *Studies in surface science and catalysis*, vol 107. Elsevier, pp 447–453
Taherian Z, Khataee A, Orooji Y (2021) Nickel-based nanocatalysts promoted over MgO-modified SBA-16 for dry reforming of methane for syngas production: Impact of support and promoters. J Energy Inst 97:100–108. https://doi.org/10.1016/j.joei.2021.04.005
Tahmasebzadehbaie M, Sayyaadi H (2022) Technoeconomical, environmental, and reliability assessment of different flare gas recovery technologies. J Clean Prod 367:133009. https://doi.org/10.1016/j.jclepro.2022.133009
Tang Y, Li Y, Bao W et al (2023) Enhanced dry reforming of CO2 and CH4 on photothermal catalyst Ru/SrTiO3. Appl Catal B 338. https://doi.org/10.1016/j.apcatb.2023.123054
Taylor P, Balat M (2008) Energy sources, part A: recovery, utilization, and environmental effects possible methods for hydrogen production:37–41. https://doi.org/10.1080/15567030701468068
Tengfei L, Cheng J, Li D et al (2024) Syngas production from photothermal synergistic dry reforming of CH4 over a core-shell structured Ni/CeO2–ZrO2@SiO2 catalyst. Int J Hydrog Energy. https://doi.org/10.1016/j.ijhydene.2024.01.004
Tolod KR, Bajamundi CJE, De Leon RL et al (2016) Visible light-driven photocatalytic hydrogen production using Cu-doped SrTiO 3. Energ Sour, Part A: Recov, Util Environ Effects 38:286–294. https://doi.org/10.1080/15567036.2013.776147
Valluri S, Claremboux V, Kawatra S (2022) Opportunities and challenges in CO2 utilization. J Environ Sci (China) 113:322–344. https://doi.org/10.1016/j.jes.2021.05.043
Velasco JA, Lopez L, Cabrera S et al (2014) Synthesis gas production for GTL applications: thermodynamic equilibrium approach and potential for carbon formation in a catalytic partial oxidation pre-reformer. J Nat Gas Sci Eng 20:175–183. https://doi.org/10.1016/j.jngse.2014.06.021
Verstraete JJ, Le Lannic K, Guibard I (2007) Modeling fixed-bed residue hydrotreating processes. Chem Eng Sci 62:5402–5408. https://doi.org/10.1016/j.ces.2007.03.020
Wang HT, Li ZH, Tian SX (2004) Effect of promoters on the catalytic performance of Ni/Al2O 3 catalyst for partial oxidation of methane to syngas. React Kinet Catal Lett 83:245–252. https://doi.org/10.1023/B:REAC.0000046083.76225.a0
Wang S, Tian Z, Liu Q et al (2018a) Facile preparation of a Ni/MgAl2O4 catalyst with high surface area: enhancement in activity and stability for CO methanation. Main Group Met Chem 41:73–89. https://doi.org/10.1515/MGMC-2018-0003
Wang S, Zhang F, Cai Q et al (2014) Catalytic steam reforming of bio-oil model compounds for hydrogen production over coal ash supported Ni catalyst. Int J Hydrog Energy 39:2018–2025. https://doi.org/10.1016/j.ijhydene.2013.11.129
Wang Y, Yao L, Wang S et al (2018b) Low-temperature catalytic CO2 dry reforming of methane on Ni-based catalysts: a review. Fuel Process Technol 169:199–206. https://doi.org/10.1016/j.fuproc.2017.10.007
Xiang D, Zhao S (2018) Parameter optimization and thermodynamic analysis of COG direct chemical looping hydrogen processes. Energy Convers Manag 172:1–8. https://doi.org/10.1016/j.enconman.2018.07.007
Xie H, Yu Q, Zhang Y et al (2017) New process for hydrogen production from raw coke oven gas via sorption-enhanced steam reforming: Thermodynamic analysis. Int J Hydrog Energy 42:2914–2923. https://doi.org/10.1016/j.ijhydene.2016.12.046
Xie T, Zhang ZY, Zheng HY et al (2022) Enhanced photothermal catalytic performance of dry reforming of methane over Ni/mesoporous TiO2 composite catalyst. Chem Eng J 429:132507. https://doi.org/10.1016/j.cej.2021.132507
Xu L, Xiu Y, Liu F et al (2020) Research progress in conversion of CO2to valuable fuels. Molecules 25. https://doi.org/10.3390/molecules25163653
Xu Y, Zhu Y, Shen P et al (2022) Production of hydrogen by steam reforming of phenol over Ni/Al2O3-ash catalysts. Int J Hydrog Energy 47:13592–13603. https://doi.org/10.1016/j.ijhydene.2022.02.097
Yan X, Lu B, Dong H, Liu Q (2023) Solar-promoted photo-thermal CH4 reforming with CO2 over Ni/CeO2 catalyst: experimental and mechanism studies. Appl Energy 348. https://doi.org/10.1016/j.apenergy.2023.121549
Yentekakis IV, Panagiotopoulou P, Artemakis G (2021) A review of recent efforts to promote dry reforming of methane (DRM) to syngas production via bimetallic catalyst formulations. App Cat B Env 296:120210. https://doi.org/10.1016/j.apcatb.2021.120210
Yi Z, Li C, Lin H et al (2023) Pyrolysis of sawdust impregnated with bio-oil of the same origin: influence of organics in bio-oil on property of biochar. Biomass Bioenergy 178:106961. https://doi.org/10.1016/j.biombioe.2023.106961
Zayer Kabeh K, Teimouri A, Changizian S, Ahmadi P (2023) Techno-economic assessment of small-scale gas to liquid technology to reduce waste flare gas in a refinery plant. Sustain Energy Technol Assess 55. https://doi.org/10.1016/j.seta.2022.102955
Zhan MC, Wang WD, Tian TF, Chen CS (2010) Catalytic partial oxidation of methane over perovskite La 4Sr8Ti12O38-d solid oxide fuel cell (SOFC) anode material in an oxygen-permeable membrane reactor. Energy Fuel 24:764–771. https://doi.org/10.1021/ef900995t
Zhang C, Li Y, Chu Z et al (2024) Analysis of integrated CO2 capture and utilization via calcium-looping in-situ dry reforming of

methane and Fischer-Tropsch for synthetic fuels production. Sep Purif Technol:329. https://doi.org/10.1016/j.seppur.2023.125109
Zhang J, Li Y, Sun J et al (2022a) Applied catalysis B: environmental regulation of energetic hot carriers on Pt / TiO 2 with thermal energy for photothermal catalysis. Appl Catal B 309:121263. https://doi.org/10.1016/j.apcatb.2022.121263
Zhang L, Wang X, Shang X et al (2017) Carbon dioxide reforming of methane over mesoporous nickel aluminate/Γ-alumina composites. J Energy Chem 26:93–100. https://doi.org/10.1016/j.jechem.2016.08.001
Zhang M, Zhang J, Wu Y et al (2019) Insight into the effects of the oxygen species over Ni/ZrO2 catalyst surface on methane reforming with carbon dioxide. Appl Catal B 244:427–437. https://doi.org/10.1016/j.apcatb.2018.11.068
Zhang X, Wang J, Song Z et al (2023) Co3O4-CeO2 for enhanced syngas by low-temperature methane conversion with CO2 utilization via a catalytic chemical looping process. Fuel Process Technol 245:107741. https://doi.org/10.1016/j.fuproc.2023.107741
Zhang Y, Wang W, Wang Z et al (2015) Steam reforming of methane over Ni/SiO2 catalyst with enhanced coke resistance at low steam to methane ratio. Catal Today 256:130–136. https://doi.org/10.1016/j.cattod.2015.01.016
Zhang Z, Zhang T, Wang R et al (2022b) Photo-enhanced dry reforming of methane over Pt-Au / P25 composite catalyst by coupling plasmonic effect. J Catal 413:829–842. https://doi.org/10.1016/j.jcat.2022.07.028
Zhao L, Tang M, Wang F, Qiu X (2023) Efficient Cu/CeO2 composites for hydrogen production from photothermal methanol steam reforming: the utility of synergism of photo and thermal catalysis. Fuel 331. https://doi.org/10.1016/j.fuel.2022.125748
Zheng H, Zhang Z, Xu K et al (2022) Analysis of structure-induced performance in photothermal methane dry reforming reactor with coupled optics-CFD modeling. Chem Eng J:428. https://doi.org/10.1016/j.cej.2021.131441
Zhong W, Wang C, Zhao H et al (2022) Synergistic effect of photothermal catalytic glycerol reforming hydrogen production over 2D Au / TiO 2 nanoflakes. Chem Eng J 446:137063. https://doi.org/10.1016/j.cej.2022.137063